

Tallinn University of Technology
School of Science
Department of Chemistry and Biotechnology

**An Investigation of the Self-Association Behaviour of Novel
Lipophilic Fluorophores in Acidic Conditions with NMR
Spectroscopy**

Bachelor thesis

Student: Kirsti Palmi
Supervisor: Jasper Adamson, National Institute of Chemical Physics and Biophysics, Senior
Research Fellow
Co-supervisor: Helena Venassa Roithmeyer, University of Zurich, Junior Research Fellow
Study program: Applied Chemistry, Food and Gene Technology

Tallinn 2022



Tallinna Tehnikaülikool
Loodusteaduskond
Keemia ja biotehnoloogia instituut

Uudsete lipofiilsete fluorofooride enese-seostumise uurimine happelistes tingimustes TMR-spektroskoopia abil

Bakalaureusetöö

Üliõpilane: Kirsti Palmi

Juhendaja: Jasper Adamson, Keemilise ja Bioloogilise Füüsika Instituut, vanemteadur

Kaasjuhendaja: Helena Vanessa Roithmeyer, Zürichi Ülikool, nooremteadur

Õppekava: Rakenduskeemia, toidu- ja geenitehnoloogia

Autorideklaratsioon

Kinnitan, et olen koostanud antud lõputöö iseseisvalt ning seda ei ole kellegi teise poolt varem kaitsmisele esitatud. Kõik töö koostamisel kasutatud teiste autorite tööd, olulised seisukohad, kirjandusallikatest ja mujalt pärinevad andmed on töös viidatud.

Autor: Kirsti Palmi
[allkiri ja kuupäev]

Töö vastab bakalaureusetööle esitatavatele nõuetele.
Juhendaja: Jasper Adamson
[allkiri ja kuupäev]

Töö vastab bakalaureusetööle esitatavatele nõuetele.
Juhendaja: Helena Vanessa Roithmeyer
[allkiri ja kuupäev]



26.05.2022

Töö on lubatud kaitsmisele.
Kaitsmiskomisjoni esimees:
[allkiri ja kuupäev]

Table of Contents

Abstract	5
Annotatsioon.....	6
Abbreviations	7
Introduction	8
1. Literature Review	9
1.1. Optical Sensors.....	9
1.1.1. Design of an Optical pH Sensor	9
1.2. Novel Lipophilic Phosphazene Based pH Indicators.....	10
1.2.1. Coumarins	11
1.2.2. Optical Properties of Novel Phosphazene pH Indicators	11
1.3. Nuclear Magnetic Resonance Spectroscopy	12
1.3.1. Brief Overview of Nuclear Magnetic Resonance Spectroscopy	12
1.3.2. Nuclear Magnetic Resonance Spectroscopy for Supramolecular Systems	13
1.4. Investigation of Dimerisation by Nuclear Magnetic Resonance Spectroscopy.....	14
1.4.1. Dimerisation of Novel Phosphazene pH Indicator Based on Structure 1a	15
2. Results and Discussion	17
2.1. Analysis of 1a in Neutral Conditions	17
2.2. Analysis of 1a in Acidic Conditions with the Addition of TfOH	18
2.2.1. Comparison of the NMR Spectra of Neutral and Protonated 1a	18
2.2.2. Chemical Shift Changes in the Experiment 2 Spectra	18
2.2.3. Evaluation of the Additional Signals in Experiment 2	20
2.2.4. Analysis of 1a in the Constantly Acidic Conditions with the Addition of TfOH	20
2.2.5. Acetonitrile and TfOH Interactions	22
2.2.6. Conclusion of the Experiments with TfOH	23
2.3. Analysis of 1a in Acidic Conditions with the Addition of HCl	24
2.3.1. Comparison of the Neutral and Protonated 1a NMR spectra.....	24
2.3.2. Spectral Changes in Experiment 6.....	24
2.3.3. Evaluation of the Additional Signals in Experiment 6	25
2.3.4. Kinetic Experiment with the Addition of HCl	25
2.3.5. Acetonitrile and HCl Interactions	26
2.3.6. Conclusion of the Experiments with HCl	27
3. Experimental	29
3.1. General Information.....	29
3.2. Experimental Procedures	29
3.3. Data Fitting with Bindfit	31
Conclusions	32
Acknowledgements.....	33
References.....	34
Appendix	38
Appendix 1. ¹ H NMR data, Spectra and Graphs	38
Appendix 2. Colour Changes During the Experiments 3 and 4	46
Appendix 3. NMR Experiment Measuring Parameters	47

Abstract

The present thesis aimed at investigation of the self-association behaviour of novel lipophilic fluorescent pH sensors with nuclear magnetic resonance spectroscopy. Optical chemical sensors, for example, molecules investigated in this thesis, have found use in many applications. One of the most essential properties of such sensors is robustness or inertness to have only limited interactions in media, as these can lead to changes in the optical properties of the molecules and thus misinterpretation of the data. In this respect, in acidic solution, as revealed by quantum chemical calculations and comparison of one- and two-photon absorption spectra of protonated novel phosphazene sensors, self-dimerisation between the molecules should be evaluated as a possible contributing factor while interpreting spectral results.

Preliminary findings from dilution series spectra suggested the possibility of self-assembly, which occurs only when the molecule is protonated by adding one drop of trifluoromethanesulfonic or hydrochloric acid. However, later discoveries of acid and acetonitrile reaction products described in this thesis prevented further quantification of the dimerisation constants from being performed and definite assumptions being made about the self-dimerisation of the molecule. Along with the result from quantum chemical calculations and optical spectroscopy, the conclusion could be made that dimerisation is an unlikely source of the observed absorption properties. A detailed presentation of the findings is undertaken in this thesis.

Annotatsioon

Käesoleva lõputöö eesmärgiks oli uurida uudsete lipofiilsete fluorestseeruvate pH indikaatorite enese-seostumist tuumamagnetresonantsspektroskoopia abil. Optilised keemilised sensorid, näiteks käesolevas lõputöös uuritud molekulid, on leidnud palju kasutust erinevates valdkondades. Selliste indikaatorite üks olulisemaid omadusi on robustsus või inertsus, omada ainult teatud interaktsioone lahuses, kuna need võivad põhjustada muutusi molekulide optilistes omadustes ja seega komplitseerida andmete tõlgendamist. Nagu näitasid kvantkeemilised arvutused ja protoneeritud uudsete fosfaseen indikaatorite ühe- ja kahefotoonsete neeldumisspektrite võrdlus, tuleks kaaluda molekulide vahelise enese-dimerisatsiooni võimalikkust.

Esialgseid leiud lahjendusseeria spektritest viitasid eneseseostumise võimalikkusele ja, et see toimub ainult siis, kui molekul on protoneeritud, käesolevas lõputöös ühe tilga trifluorometaansulfoon- või vesinikkloriidhappe lisamisega. Hilisemad avastused happe ja atsetonitriili reaktsiooniproduktidest ei võimaldanud arvutada dimerisatsioonikonstante ega teha lõplikke järeldusi molekuli dimeriseerumise kohta. Võttes arvesse ka kvantkeemiliste arvutuste ja optilise spektroskoopia tulemused on molekulide vaheline dimerisatsioon ebatõenäoline täheldatud absorptsiooniomaduste allikas. Detailne tulemuste kirjeldus on toodud käesolevas lõputöös.

Abbreviations

2PEF	two-photon excitation fluorescence
1PA	one-photon absorption spectra
2PA	two-photon absorption spectra
NMR	nuclear magnetic resonance spectroscopy
HG	host-guest complex
FID	free-induction decay
UV	ultraviolet
Vis	visible
DFT	density functional theory
COSY	correlation spectroscopy
SI	supporting information
TfOH	trifluoromethanesulfonic acid

Introduction

Scientific developments in many fields, such as in medicine, biochemistry, marine biology, and others, have connected the pH change of the investigated system to various pathologies, which brings about a growing interest in advancing pH measuring techniques. One of the proposed approaches to improving pH sensing is the use of optical chemical sensors, which has been a growing area of interest over the last four decades and has found a broad range of applications in real-life uses, such as detecting various metal ions in cells.^{1,2}

One family of such chemical pH sensors was synthesised by Selberg and colleagues by linking the 7-amino-4-(trifluoromethyl)coumarin backbone to the phosphazene with different substituents.³ One of the possible applications of these indicators was in two-photon excitation fluorescence microscopy. However, investigations of the two-photon absorption properties of the protonated molecules and quantum chemical calculations led to the hypothesis that these novel pH sensors could self-dimerise.⁴ The potential self-association between the indicator molecules was investigated by nuclear magnetic resonance spectroscopy, which built the foundation of this thesis. The results were published in the scientific paper *Chemistry – A European Journal* (found in the Ref. [4]) in cooperation with the research group of Professor Aleksander Rebane. The main objectives of the research were to determine any possible aggregation, specifically, dimerisation, of the compound, after protonation as aggregation or interaction between sensor molecules could alter the data or cause misinterpretation of the pH value when used in optical systems.

The thesis includes a literature overview of optical sensors and the research method, results and discussion, and an experimental part.

1. Literature Review

1.1. Optical Sensors

pH is among the most widely used and essential chemical parameters in many scientific fields. One of the oldest methods of pH detection involves universal indicators consisting of multiple compounds with several colour changes in the pH scale, which are added straight to the investigated solution or impregnated on a reagent paper.⁵ The scale of pH, which is known today, was first described by a Danish chemist Søren Sørensen in 1909, who needed a scale to compare the acidity of the beer. He defined it as a negative logarithm of the concentration of the hydronium ions, while nowadays, its activity is used instead.²

The most common pH measuring technique currently involves a combination electrode combining a reference electrode such as Ag/AgCl and a glass membrane electrode.² The glass electrode and its applications were first presented in 1909 by Haber and Klemensiewicz, who used a sterilised and moisturised (soaked in distilled water) glass bulb to measure the titration curve of HCl-NaOH.⁶

Electrochemical methods provide the fastest and most accurate results in pH analysis. However, as pH measurements have become more important in the field of medicine for detecting various pathologies, such as drug resistance, cancer, or Alzheimer's disease⁷, some technical disadvantages are experienced with typical electrochemical methods. Examples of these are electrical interferences, the necessity of calibration or reference electrodes and the inability to measure in small systems like cells due to the comparably large size of the electrode. Moreover, with human tissue monitoring, blood pH levels can drastically change over a matter of minutes. Thus, the current method, where the blood needs to be drawn from the patient and remotely analysed, is unable to predict or warn about the patient condition in advance.⁸

Challenges in pH detection applications in various fields have brought scientists' attention to developing optical sensing methods.^{5,8} Optical chemical sensors are usually weak acids or bases with characteristic optical properties in their protonated or deprotonated forms.⁹ The particularly interesting and valuable aspect of these sensors is that they provide real-time information about the investigated compound or ions through direct or reagent-mediated detection.^{1,10} The direct sensors detect the change in the optical properties of the analyte, for example, absorption, luminescence, or fluorescence intensity, whereas reagent-mediated systems measure the response of the analyte-sensitive indicator molecule.^{1,2}

1.1.1. Design of an Optical pH Sensor

The indicator is most often immobilised on or encapsulated in a solid or liquid phase matrix permeable to the analyte in the optical sensor systems. Solid matrices like sol-gels or polymer membranes are commonly used in the reagent-mediated sensors used for pH sensing. The matrix plays an important role in the effectiveness of the system as the sensor design itself since the matrix can alter the properties of the probe.^{1,5} Its functions include proton diffusion facilitation and providing the sensor with chemical, mechanical and thermal stability.^{2,5}

The design of the optical pH sensor is not a trivial matter. There are many requirements to consider when constructing the indicator, such as the pK_a value, lipophilicity for uses in biochemistry, chemical stability and photostability, and spectral properties like high extinction coefficient and absorption/excitation and emission band in the visible region. The last is essential for reducing the photobleaching effect and enabling the use of low-cost optical components and light sources.^{2,5} What is more, sensors for pH detection in the biological matter should present their optical features in the red/infrared region because this region exhibits low background noise from other biological molecules.² Also, membrane-specific probes are expected to have lipophilic moieties to ensure compatibility with the lipid bilayer structures.

Although many acid-base sensors have been described in the literature², they exhibit complications when used in non-polar membranes. One of the significant disadvantages is that they present well-defined charged groups in their charged states, which causes leaching out of the membranes due to their hydrophilic nature. Moreover, they are prone to molecular interactions and have a limited pH detection range.⁵

All these considerations were taken into account by Sigrid Selberg et al.³ in 2019, who aimed to synthesise a new family of optical pH sensors with high lipophilicity of both neutral and charged forms. In addition to that, the indicators were aimed to lack localised charges in the protonated forms and have spectral changes upon (de)protonation, which are observed in the visible spectral range or even have strong fluorescence.^{3,5}

1.2. Novel Lipophilic Phosphazene Based pH Indicators

To fulfil the requirements mentioned above, Selberg et al.³ used 7-amino-4-(trifluoromethyl)coumarin as a backbone and phosphazene with different constituents to design novel fluorescent pH indicators presented in Figure 1. The synthesised indicators contained various functional groups like phosphazene for basicity and a lipophilicity centre with phenyl and pyrrole constituents for charge delocalisation, making it possible to create a group of sensors with different pK_a values. In addition, coumarin was used as an absorbing and fluorescing moiety.

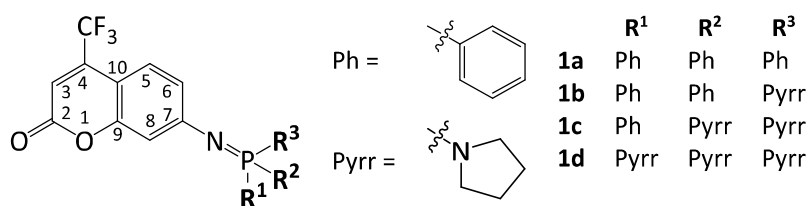


Figure 1. Structures of the fluorescent lipophilic pH sensors synthesised by Selberg et al.³ where different phosphazenes are attached to the 7-amino-4-(trifluoromethyl)coumarin backbone.

Contrary to coumarins, phosphazenes have not been extensively used in molecular sensor systems despite their excellent chemical stability and availability.^{5,11} In the phosphazenes, the nitrogen atom is connected to the phosphorus atom by a double bond. The behaviour of the double bond is similar to the phosphorus ylides; it can be present in the form of an ylene with a formal double bond or an ylide with two opposing charges, where the phosphorous atom has a partial positive, and the nitrogen atom has a partial negative charge. The general understanding is that the ylide form contributes more to the resonance hybrid.¹²

The ylide character of the nitrogen-phosphorous bond made it possible to have significant electron delocalisation into the aromatic core of the coumarin. Also, the partial negative charge of the imino nitrogen functions as a protonation site.⁵

1.2.1. Coumarins

Coumarins, fused from benzene and α -pyrone ring¹³ (Figure 2), are a widely investigated class of naturally occurring molecules, first isolated from the tonka beans (*Coumarou*) by Vogel in 1820¹⁴. Currently, around a thousand coumarins have been described as secondary metabolites from various plants, fungi, and bacteria, with the most important families *Rutaceae* (citrus) and *Umbelliferae* (celery, carrot, or parsley).^{13,15}

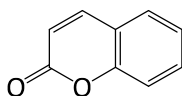


Figure 2. Structure of the coumarin, 2H-1-Benzopyran-2-one.¹³

The correct structure for coumarin was proposed in 1867 by Stecker.¹⁶ The coumarin scaffold consists of an aromatic planar ring of lipophilic nature, which is described to interact via π - π stacking in many biological systems. Moreover, the lactone moiety offers a strong polar binding site for hydrogen-bonding and dipole-dipole interactions.¹⁵ Shortly after that, William Henry Perkin developed the first synthesis pathway, known as the Perkin reaction consisting of numerous condensation reactions to afford the coumarin molecule.^{16,17}

Coumarins gained interest due to their wide range of applications in various scientific fields, including pharmacology, cosmetics, and food production.^{18,19} One of the great attributes of coumarins are their optical properties, such as photostability and high quantum yields, which justify their application as fluorescent probes.¹⁸ The coumarin core has been used to develop sensors for cyanide detection in water²⁰, pH^{3,21,22} and detection of metal ions such as mercury²³, copper²⁴, magnesium²⁵ or zinc²⁶ in cells.

1.2.2. Optical Properties of Novel Phosphazene pH Indicators

The initial characterisation of the photophysical properties of the novel phosphazene pH indicators was conducted by Selberg et al.³ In addition, the authors were interested in the two-photon absorption properties of the molecules for applications in biology and medicine through high-resolution functional microscopy.

Two-photon excitation fluorescence (2PEF) microscopy is an imaging method where two photons are used for the excitation of a fluorophore instead of one, as is used in linear one-photon microscopy, whereas the energy of photons in two-photon absorption (2PA) transition is half of the energy of the photon in respective one-photon absorption (1PA) transition (Figure 3). The technique is less sensitive to light scattering, offers reduced photobleaching and deeper tissue penetration up to one millimetre.²⁷

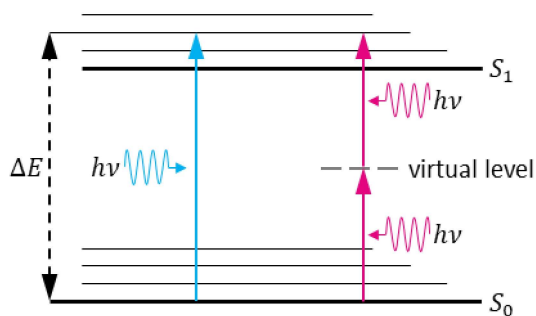


Figure 3. Illustration of one-photon (marked in blue) and two-photon (marked in pink) transition from ground state S_0 to first excited state S_1 . ΔE represents the energy difference between the ground and first excited state, h - Planck's constant and ν - frequency of the photon. Dashed grey line depicts a virtual intermediate state.^{28,29}

Matt Rammo et al.³⁰ conducted extensive 2PEF experiments with neutral and protonated forms of the phosphazene based sensors to determine their 2PEF properties (the detailed description of experimental methods and results can be found in the Ref. [28]). However, when comparing the 1PA and 2PA spectra of the protonated forms of the molecules, they found a mismatch between the absorption maxima and line shape.⁴ It is generally expected that the 1PA and 2PA spectra should have a close match.³¹ This observation, along with the quantum chemical calculations performed by Merle Uudsemaa and Aleksander Trummal led to the idea that the investigated phosphazene sensors can form dimers upon protonation at high concentrations. This assumption was investigated by nuclear magnetic resonance spectroscopy (NMR), which built the foundation of this thesis.⁴ The investigations of molecules' self-association behaviour were necessary for their potential applications as pH sensors as any interaction or aggregation can lead to faulty data and misinterpretation of pH.

The following paragraphs will discuss NMR spectroscopy in supramolecular chemistry, an experimental technique used to characterise the self-association of the compound and dimerisation.

1.3. Nuclear Magnetic Resonance Spectroscopy

1.3.1. Brief Overview of Nuclear Magnetic Resonance Spectroscopy

NMR spectroscopy is a non-destructive method for structural elucidation of chemical species based on nuclear spins. Its history goes back to the 1920s when Wolfgang Pauli suggested that nuclei have spin angular momentum and therefore possess magnetic moments.^{32,33} From the discovery of the magnetic moments, many other developments in the method have brought numerous Nobel Prizes in physics and later its applications in chemistry and medicine.³⁴

The concept of NMR is based on a theory that atomic nuclei have spin-rotation around one's axis. The same applies to protons and neutrons, which form the atomic nuclei as well as the electrons in the atoms. When spins of the protons and neutrons in the nuclei are not paired, the nuclei are said to possess charge, and rotation around the axis creates a magnetic field. Therefore, only nuclei with non-zero spin are NMR active and can be measured.³⁵⁻³⁷ For example, one of the most common isotopes measured with NMR is ^1H , with a spin quantum number of $\frac{1}{2}$ and a natural abundance of 99.98 %. Whereas carbon isotope ^{12}C , a typical atom found in organic molecules, is NMR inactive,

having a spin quantum number of zero. Alternatively, ^{13}C is used instead with a spin quantum number of $\frac{1}{2}$, although due to its low natural abundance, of only 1.11 %, higher concentrations are desirable.

In all molecular spectroscopy methods, the interest lies in the energy transfer from a photon to a molecule. In NMR, it is the energy difference between the spin-states. A nucleus with a spin quantum number $\frac{1}{2}$ has two spin-states, α with a value of $+\frac{1}{2}$ and β with a value of $-\frac{1}{2}$ (Figure 4). As there is no difference between the energies of the two spin-states, the probability that the nucleus is in either one is equal. However, absorption of the energy from a photon can only occur when the spin-states differ in energy (ΔE). This is generated by orienting magnetic moments of a nucleus in one of the two directions when it is placed in the external magnetic field B_0 .^{36–38}

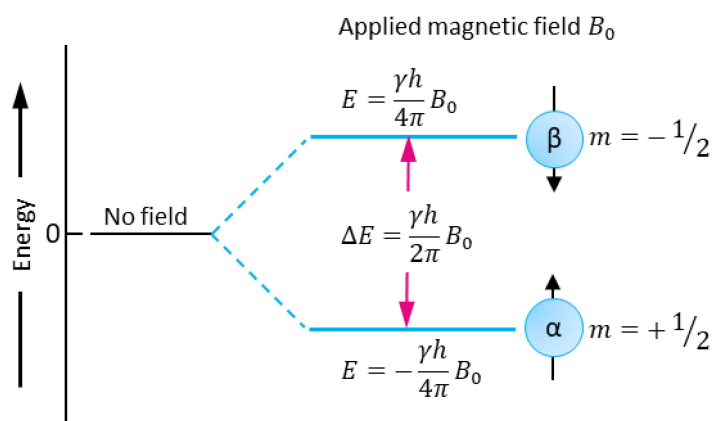


Figure 4. Energy levels and magnetic moments for a nucleus with a spin quantum number of $\frac{1}{2}$. ΔE represents the energy difference between the spin-states and is proportional to the strength of the applied magnetic field, where γ – gyromagnetic ratio, h - Planck's constant and B_0 is the strength of the applied magnetic field.^{36–38}

When nuclei in the lower energy state in the external magnetic field are exposed to electromagnetic radiation with a radio frequency that exactly matches ΔE , they are excited to the higher energy spin-state. The relaxation to the lower energy state is saved as free-induction decay (FID) when the NMR spectra are recorded. Fourier transformation is used to convert the FID, which is in the time domain and complicated to interpret, to the frequency domain, which gives the NMR spectrum.^{12,36,37}

1.3.2. Nuclear Magnetic Resonance Spectroscopy for Supramolecular Systems

NMR has found great significance in a broad range of applications in chemistry, biochemistry, and in medicine as magnetic resonance imaging. Its ability to describe the environment of atomic nuclei in the molecular and complex structures is utilised in the supramolecular chemistry to provide information about the regions of the molecule which take part in complex formation and to describe the symmetry of components and aggregates.³⁹

In supramolecular chemistry, the interest lies in the complex formation of the host, usually a larger molecule, and guest(s) via noncovalent interactions. These chemical machines have found many real-life applications, such as chemical sensing of blood ion concentrations or continuous glucose monitoring, metal extraction from ores, and drug delivery or removal to/from the human body.⁴⁰

One significant property in all the applications is the binding constant, which provides information about the affinity of the host towards a certain guest.⁴¹

One of the methods to determine the binding constant of the HG complex are NMR titrations, where the host concentration is kept constant through the experiment, and guest concentration is gradually increased. As the chemical shifts of the individual host and guest are different from the chemical shifts of the host and guest in complex, the binding constant can be calculated based on a single ¹H NMR titration experiment. In the fast exchange kinetic systems, where chemical shifts are the weighted averages of the free and bound host, the binding constant can be calculated from the data gained from the titration experiment.⁴²

In addition to the binding constants, NMR titration experiments could give information about the structure of the HG complex as the atoms in the interacting functionalities experience the most significant chemical shift changes.⁴²

Self-association is a process whereby two of the same molecules interact with each other. For example, similarly to host-guest binding, a molecule can form a dimer with itself. NMR allows to determine the binding characteristics and strengths of this association, similarly to host-guest binding of two different species.

1.4. Investigation of Dimerisation by Nuclear Magnetic Resonance Spectroscopy

Dimerisation is one of the phenomena investigated in supramolecular chemistry alongside host-guest processes, molecular devices, and machines.⁴³ Supramolecular chemistry has been described as “chemistry beyond the molecule”⁴⁴, referring to the fact that compounds are constructed by linking them with intermolecular forces, such as hydrogen or halogen bonds, π - π interactions etc.⁴⁵

The strength of the self-association in the dimer is described with the dimerisation constant, which explains the monomer-dimer equilibrium in the system. Dimerisation could be expressed with the following equation:



$$K_d = \frac{[D]}{[M]^2}, \quad (2)$$

where M is the monomer, D is the dimer, $[M]$ and $[D]$ are their molar concentrations; K_d is the dimerisation constant.^{46–48}

With the ¹H NMR, there is a possibility to determine the dimerisation constants in the solution-state by measuring the changes in the chemical shifts via serial dilution.⁴⁹ With the dilution, it is expected that the monomer concentration increases whereas the dimer concentration decreases.⁵⁰

In the molecular systems where the monomer-dimer equilibrium has fast exchange kinetics compared to the NMR time scale, the observed chemical shift of the signal is a weighted average of the monomer and dimer chemical shifts.⁵¹ This observed chemical shift (δ_{obs}) can be expressed by the following equations (3-5):

$$\delta_{obs} = \chi_m \delta_m + \chi_d \delta_d = \delta_m + (\delta_d - \delta_m) \chi_d \quad (3)$$

$$\chi_m + \chi_d = 1 \quad (4)$$

$$[M]_0 = [M] + 2[D], \quad (5)$$

where δ_m and δ_d are monomer and dimer chemical shifts; χ_m and χ_d are mole fractions of the monomer or dimer form; $[M]_0$ is the total concentration.^{47–49,52}

Using the equations (3-6) in the dimerisation constant calculations, the monomer-dimer equilibrium can be stated as:⁵²

$$K_d = \frac{(\delta_d - \delta_m)(\delta_{obs} - \delta_m)}{2(\delta_d - \delta_{obs})^2 [M]_0}. \quad (6)$$

Nowadays, specialised fitting programs are created to determine the binding constants for different supramolecular systems and spectroscopy methods. For example, Bindfit from *supramolecular.org*, which Professor Pall Thordarson founded in 2015.^{53,54}

1.4.1. Dimerisation of Novel Phosphazene pH Indicator Based on Structure 1a

NMR spectroscopy studies of the assumed self-assembly of the fluorophores synthesised by Selberg et al.³ were conducted based on the molecule variant **1a** (Figure 1) due to three equal phenyl substituents attached to the phosphazene moiety preventing complicated structure analysis of the asymmetric substituents. The molecule exhibits an extended conjugated π -electron system enlarged by the phosphazene constituent.³⁰

The resonance structures of compound **1a** coumarin moiety are presented in Figure 5. The nitrogen atom is donating its lone pair of electrons to the π -electron system of the coumarin function.⁵⁵ The conjugation of the system increases the electron density on the carbon atoms in positions 3, 6, 8 and 10, giving them partial negative charges. As a result, the electron density near the hydrogen atoms attached to the carbon atoms also increases, which causes a shielding effect resulting in an upfield shift in the ^1H NMR spectrum.³⁸ Phenyl groups attached to the phosphazene moiety are expected to have higher downfield chemical shifts due to the deshielding effect of the ring current.³⁸

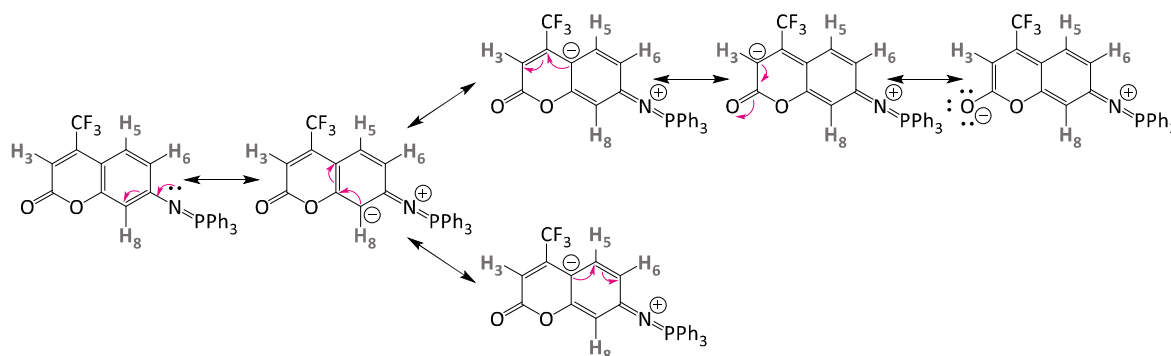


Figure 5. Resonance structures of **1a** with the designation of its protons by numbers.

The molecule has two possible protonation sites: carbonyl oxygen on the coumarin moiety and the nitrogen atom linking the phosphazene and coumarin functions. Quantum chemical calculations have shown that the preferred protonation site is nitrogen (Figure 6).^{3,30} Upon protonation, the

conjugation in the molecule is diminished⁴ as the nitrogen does not have a lone pair of electrons to donate to the π -system. The diminished conjugation between the coumarin moiety and the linking nitrogen atom ought to cause downfield chemical shifts for the hydrogen signals H₃, H₆ and H₈ due to the decreased electron density compared to the neutral molecule.³⁸

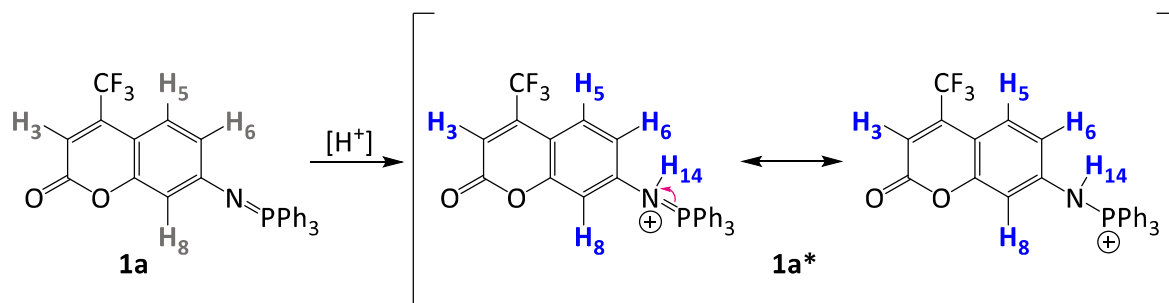


Figure 6. The structure of the variant **1a** of the fluorescent lipophilic pH sensors synthesised by Selberg et al.³ and its resonance structures after protonation.

The other process suggested upon protonation at higher concentrations is homodimerisation via hydrogen bond formation. The hydrogen atom attached to the nitrogen atom functions as a hydrogen bond donor and the carbonyl oxygen as an acceptor in the dimer.⁴ In this process, the oxygen atom donates part of its electron density to the nitrogen atom through a hydrogen bond and the *ortho*- and *para*- positions to the nitrogen atom become richer in electron density.⁵⁵ This causes H₆ and H₈ upfield positions compared to the protonated monomeric compound in the ¹H NMR spectra.

Two possible structures of the protonated **1a** dimers are illustrated in Figure 7. When looking at the dimer in Figure 7a, it is expected to observe one set of chemical shifts for each proton in the molecule since the electronic environment for the protons in both monomers is the same – the dimer is symmetrical. Whereas in the case of the dimer in Figure 7b, two signals for every proton would be expected. This is due to the different electronic environments of the hydrogen bond donor and acceptor monomers participating in the dimer formation. In the acceptor, the monomer chemical shifts are assumed to appear more upfield compared to the donor molecule.³⁸

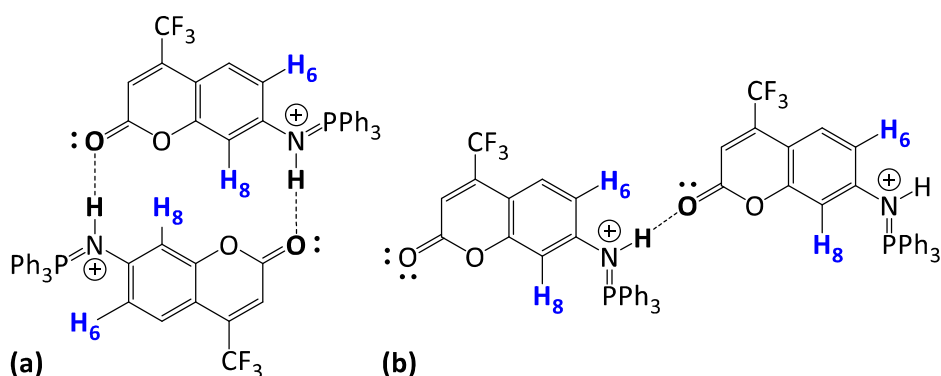


Figure 7. Two of the possible dimer structures for protonated **1a**.

2. Results and Discussion

The research aimed at investigation of possible self-association, specifically dimerisation, of the novel lipophilic pH sensors synthesised by Selberg et al.³ with NMR spectroscopy. With an original hypothesis from the results of 1PEF and 2PEF experiments and quantum chemical calculations, the thesis set to explore whether dimers can form in solution when the samples are acidified. To achieve this, compound **1a** was chosen as a model compound for the serial dilution experiments conducted in neutral and acidic conditions, where trifluoromethanesulfonic acid (TfOH) or hydrochloric acid (HCl) were used as an acidifying agent in the acetonitrile-*d*₃ (CD₃CN) solution. Chemical shift changes and movement direction of the **1a** proton signals were monitored as an indication of the protonation and self-dimerisation, paying particular attention to the signals H₃, H₆ and H₈ as these are most affected by conjugation of the nitrogen and carbonyl group in the structure of **1a**. During the present study, discoveries of the acid and CD₃CN solvent reaction products were discovered. The performed work was therefore focused on understanding these acid-solvent interactions.

The NMR experiments presented below are numbered, and italic capital letters denote additional signals not seen in the neutral compound spectra for clarification.

All experiments were conducted under the supervision of senior research fellow Jasper Adamson, PhD and junior research fellow Helena Vanessa Roithmeyer, PhD.

2.1. Analysis of **1a** in Neutral Conditions

Investigations of possible aggregation of novel fluorescent pH sensor **1a** began with the experiment in neutral conditions to prove the assumption that self-association occurs only in acidic conditions and to have a reference spectrum for later uses to demonstrate that adding an acid to the sample protonates the molecule.

¹H NMR measurements of dilution series in neutral conditions (experiment 1) were conducted with **1a** in CD₃CN at 298 K. Dilutions of the samples were carried out in a way where a defined amount (specified in Appendix 3, Table 5) of the previously measured sample was transferred into a new NMR tube and diluted with CD₃CN to a specific concentration (concentrations are found in Appendix 3).

A comparison of the dilution series spectra (Appendix 1, Figure 22) did not show significant chemical shift changes for the signals of compound **1a**, indicating that the self-assembly does not occur between neutral molecules. As well as that, traces of the solvents used in the synthesis and previous analysis methods were detected. The residual solvent signals were identified by comparing experimental data to the ¹H NMR measurements conducted by Selberg et al. during the synthesis and presented in the SI of the paper.³ Traces of water, toluene, and chloroform were discovered (Figure 8).

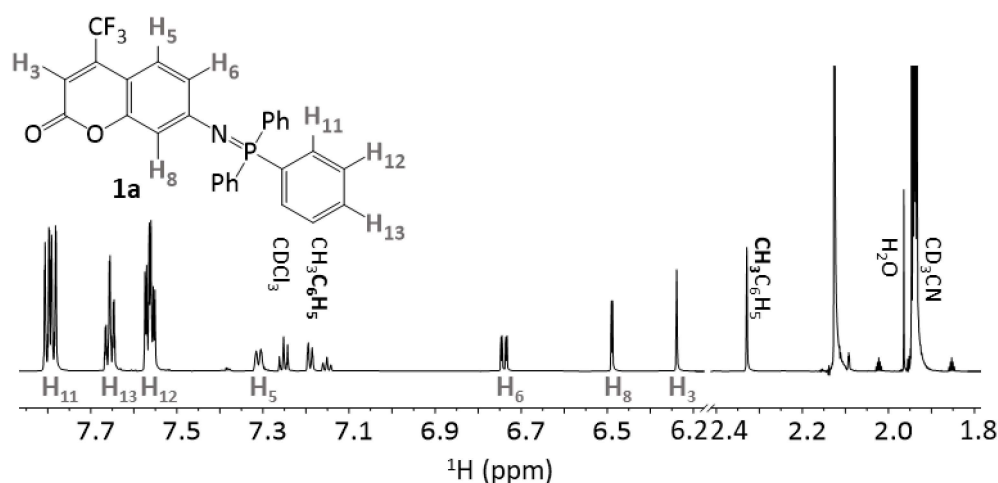


Figure 8. ^1H NMR spectrum of experiment 1 at 4.01 mM **1a** in CD_3CN at 298 K. The proton signals of **1a** are marked in grey. The assignment of the signals to the protons of compound **1a** was based on the correlation spectroscopy (COSY) spectrum (Appendix 1, Figure 20).

2.2. Analysis of **1a** in Acidic Conditions with the Addition of TfOH

2.2.1. Comparison of the NMR Spectra of Neutral and Protonated **1a**

It was noticeable that the acidified sample of **1a** (Figure 9b) resulted in significant downfield chemical shifts compared to the neutral condition spectra (Figure 9a). This corresponds to the assumption described earlier that the conjugation is diminished upon protonation due to the decrease of the nitrogen atom's ability to donate its lone pair of electrons in the aromatic systems. Thus, protons in the coumarin moiety of the protonated molecule experience higher deshielding effects.

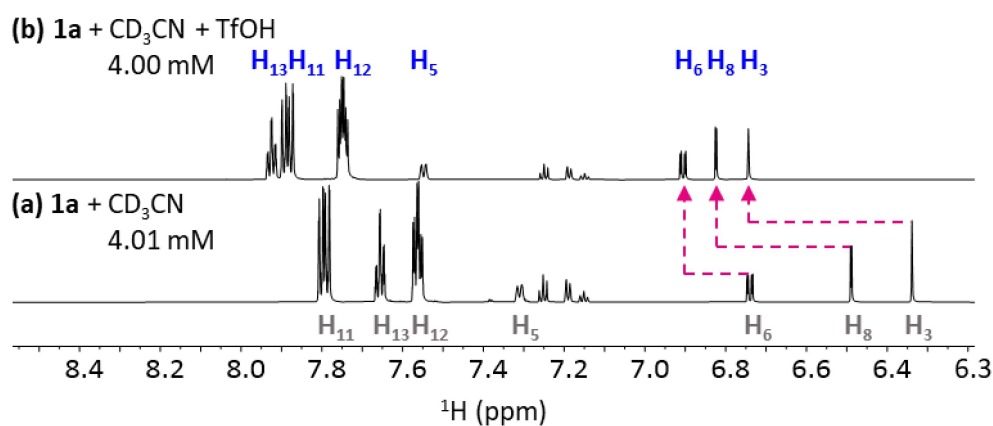


Figure 9. ^1H NMR spectra of **1a** in CD_3CN : (a) of experiment 1 at 4.01 mM spectrum at 298 K, (b) of experiment 2 at 4.00 mM spectrum acidified with a drop of TfOH, at 293 K. The proton signals of **1a** are marked in grey and **1a*** in blue. Pink arrows indicate signals downfield shifts due to protonation.

2.2.2. Chemical Shift Changes in the Experiment 2 Spectra

After investigating the **1a** in neutral conditions, the dilution experiments were repeated with TfOH to monitor chemical shift changes, suggesting possible dimerisation between the molecules under these conditions. To perform the measurements of experiment 2 in acidic conditions, samples were

prepared in the same manner as in experiment 1. However, before the first ^1H NMR measurement, one drop of TfOH was added to the NMR tube (Appendix 3, Table 5).

Upon acidification, the experiment 2 dilution series spectra showed significant chemical shift changes for protons H_6 , H_8 , and H_3 (Figure 16). It was noticed that for the first six experiments (until 1.32 mM), the chemical shifts for the investigated protons moved in one direction and then in the opposite direction. Changes in the initial chemical shifts can be rationalised by the changes in the electron density upon dimerisation.

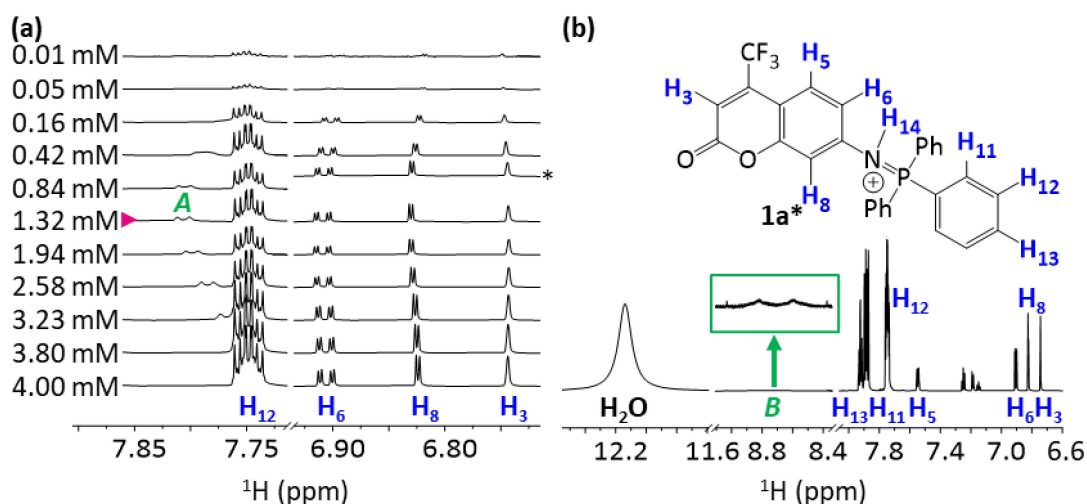


Figure 10. ^1H NMR spectra of experiment 2 of **1a** in CD_3CN acidified with one drop of TfOH at 293 K: (a) stacked spectra of the serial dilutions with a zoom to the areas of interest, (b) the full spectrum at 4.00 mM. The proton signals of **1a*** are marked in blue and additional signals not seen in the neutral spectra (**1**) are marked in green. *Spectrum with a concentration of 0.84 mM, deformation of the spectra is caused by shifting water signal.

As previously described (Figure 7), upon dimerisation, the conjugation in the coumarin moiety is partially restored as the carbonyl oxygen donates its electron density to the nitrogen atom via hydrogen bonding and from there to the π -system into *ortho*- and *para*- positions, explaining the H_6 and H_8 upfield shifts compared to the protonated monomer. Signal H_3 , on the other hand, moved in the opposite direction from signals H_6 and H_8 . In the more concentrated samples, where we expect the dimer to form, the signal appears more downfield compared to the less concentrated (1.32 mM) sample. This can be explained by the decreasing electron density around the carbonyl oxygen when the dimer is formed via hydrogen bond formation.

In addition, due to the fact that there is only one set of signals observed in the ^1H NMR spectra, the dimer is most likely associated with the structure depicted in Figure 7a.

Upon gradual dilution, dissociation of the dimer to protonated monomer is expected. For the signals H_6 and H_8 , it was observed as downfield and for the H_3 upfield chemical shifts between the concentrations of 4.00 to 1.32 mM. As the dimer dissociates, the NMR spectra correlate more with the protonated monomer spectra, where the conjugation of the molecule is diminished. At 1.32 mM, it is estimated that there are mostly protonated monomers present in the sample.

From a specific concentration (1.32 mM) in the dilution series (Figure 10a – marked with a pink arrow), signals moved in the opposite direction from the initial change. This is caused by two intertwined factors, which reduce the likelihood of dimer formation. Firstly, the acidity of the samples gradually changed over the dilution series, which was observed by the chemical shift changes of the water signal (Appendix 1, Figure 24). Secondly, fewer coumarin molecules were available for self-assembly due to the dilution. These factors occurred due to the design of the experiment, where the acid was added only to the first sample, and the following samples were diluted. This caused the previously acidic samples to turn less acidic, and fewer molecules were protonated, thus decreasing dimerisation. According to the literature, protonation is the crucial element for **1a** dimerisation.⁴

These two factors were changing the NMR spectra in the diluted samples in a way that was more in agreement with the chemical shifts of the neutral monomer of the compound rather than the dimer or protonated monomer, which means that the nitrogen atoms' ability to donate its electron density to the aromatic system was significantly increased and therefore conjugation in the molecule was restored. This correlated with H₆ and H₈ upfield and H₃ downfield shifts observed in the experiment 2 spectra.

2.2.3. Evaluation of the Additional Signals in Experiment 2

In the stacked spectrum of experiment 2 (Figure 10a), one could observe signal A, which was not present in the experiment with the neutral compound (Figure 8). Moreover, an overlap and shift of the signal from H₁₂ were observed. Integration of the H₁₂ peak in the 4.00 mM spectrum (Figure 10b) indicated the presence of seven protons, whereas, in the 1.32 mM spectrum, where A was shifted downfield in comparison to H₁₂, it showed six. The signal A with an integration of one is estimated to belong to the proton H₁₄ attached to the nitrogen atom.

Additionally, when the spectrum of **1a** with TfOH (Figure 10b) was compared to the neutral solution spectrum, a signal B was noticed in the 8.37–9.03 ppm range. The signal was assumed to belong to amide, which was confirmed later to belong to protonated acetamide (Figure 14).

2.2.4. Analysis of **1a** in the Constantly Acidic Conditions with the Addition of TfOH

In the previous experiment (Figure 10), compound **1a** was observed to undergo multiple chemical processes, such as dimer dissociation and deprotonation, due to dilution and, consequently, acidity changes to neutral (Appendix 1, Figure 24). Moreover, additional signals not seen in the neutral experiment spectra were observed. Thus, we could not determine the dimerisation constant from the obtained data.

The NMR experiment 3 was undertaken to prevent acidity changes during the dilution series. In this experiment, the stock solution was prepared from **1a** and CD₃CN, and a certain amount (specified in Appendix 3, Table 6) was transferred into NMR tubes and diluted to the desired concentration. Before the measurements were conducted, a drop (2.5 µl) of TfOH was added to each tube.

In Figure 11b, the chemical shift of the water/acidic proton varies widely over the dilution series, indicating that the samples did not have uniform acidic conditions. Constant acidity was especially important as the previous experiment showed that chemical shifts of the compound signals

correlate with acidity. For example, signal H_8 shifted upfield in the more acidic conditions (concentrations 2.10 and 4.14 mM) than in less acidic (Figure 11a). Signal A previously assigned to the H_{14} proton (Figure 11b) of the compound, and H_3 behaved similarly.

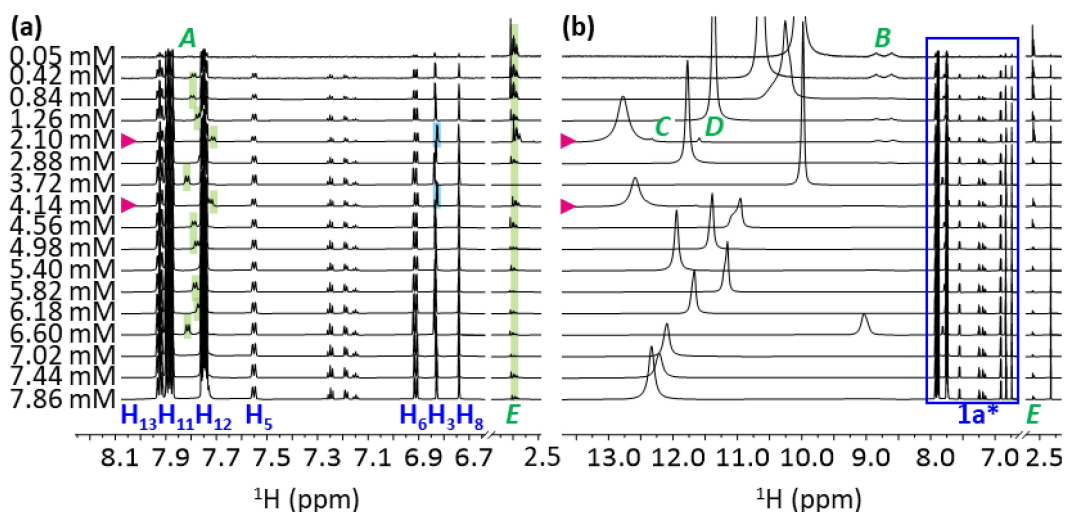


Figure 11. ^1H NMR spectra of experiment 3 of **1a** in CD_3CN acidified with $2.5\ \mu\text{l}$ of TfOH at 298 K: (a) stacked spectra of the serial dilutions with a zoom to the areas of interest, (b) full stacked spectra of the experiment. The proton signals of **1a*** are marked in blue and additional signals not seen in the neutral spectra (**1**) are marked in green. Pink arrows indicate the samples with the highest acidity.

Furthermore, in Figure 11b, additional signals *C*, *D* and *E* (signal shape can be seen in Appendix 1, Figure 27) are observed. The singlets *C* and *D* were characteristic of more acidic samples, whereas the multiplet *E* exhibited a higher intensity in the more diluted samples. These observations indicated that the solvent and the acid reacted in the NMR tube. As the dilution series measurements were conducted from the highest to the lowest concentration, the last sample had more time and acid to react and thus exhibited higher intensity than the peaks observed for the reaction of product *E*.

As the acid concentration in the samples was not constant, an NMR experiment (4) was undertaken to unify the sample acidity across the dilution row. Therefore, another $7.5\ \mu\text{l}$ of TfOH was added to each sample in NMR tubes. As seen from the spectra (Figure 12b), consistent acidity was achieved. On the other hand, adding more acid significantly increased the number of additional signals (Figure 12a) and, therefore, side reactions, which was also apparent in the form of a colour change of the samples. Moreover, previously colourless samples turned yellow, followed by red. With the colour changing to red, the viscosity of the sample changed to having sticky consistency (see Appendix 2, Figure 32).

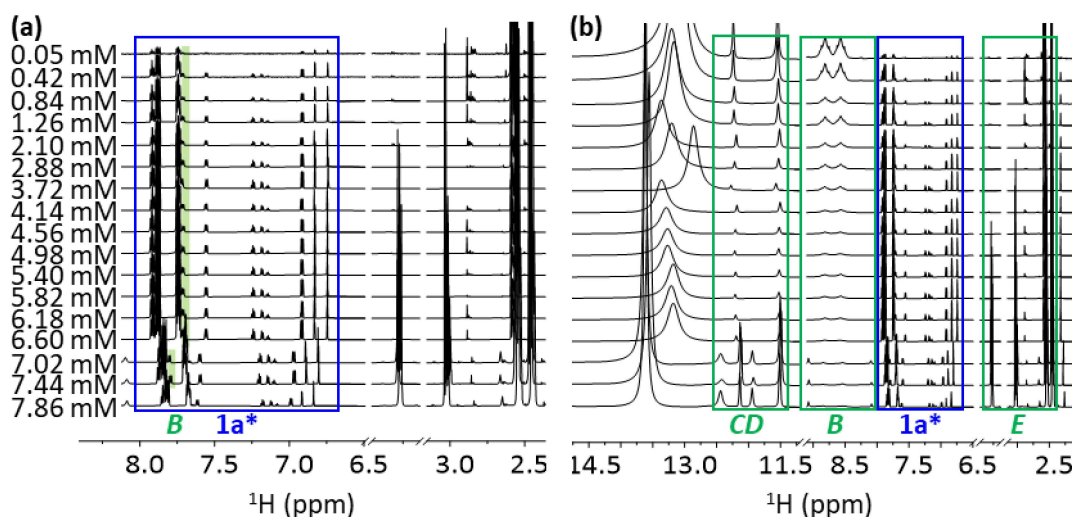


Figure 12. ^1H NMR spectra of experiment 4 of **1a** in CD_3CN acidified with $10\ \mu\text{l}$ of TfOH at 298 K: (a) stacked spectra of the serial dilutions with a zoom to the areas of interest, (b) full stacked spectra of the experiment. The proton signals of **1a*** are marked in blue and additional signals not seen in the neutral spectra (**1**) are marked in green.

In experiment 4 spectra depicted in Figure 12, it was observed that the signals of **1a** did not undergo significant chemical shift changes upon dilution in constantly acidic conditions. This could indicate that the additional compounds forming from acid and solvent reactions do not significantly affect the chemical environment experienced by the **1a** molecules. However, the magnitude of the factors affecting the **1a** chemical signals cannot be deduced from experiments conducted in this thesis.

2.2.5. Acetonitrile and TfOH Interactions

Investigations of the solvent and TfOH interactions with NMR were critical for understanding and explaining the origin of the additional signals and their association with the novel fluorophores.

From Figure 13, where TfOH and CD_3CN solution spectra are depicted, the conclusion can be made that all the additional signals in the previous spectra with **1a** and colour changes in the samples arise from TfOH and CH_3CN interactions. Extensive research about a wide variety of reaction products in CH_3CN and TfOH solution was done by George E. Salnikov et al.⁵⁶ in 2012. The formed compounds could interact with each other, be protonated, or decompose over time. The exact composition and ratio of the reaction products in the sample varies due to the acid and solvent ratios.⁵⁶

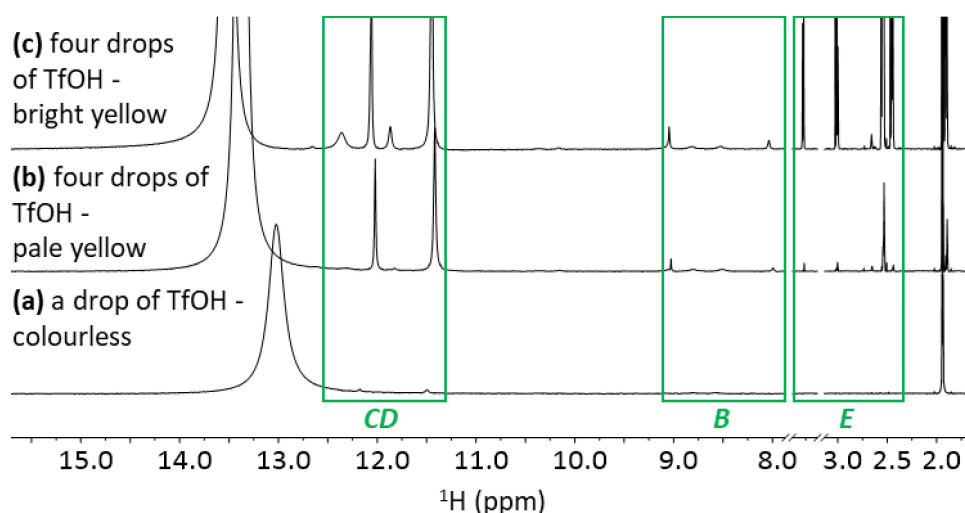


Figure 13. ^1H NMR stacked spectra of experiment 5 of CD_3CN acidified with TfOH at 298 K: solvent is acidified with (a) a drop of TfOH (colourless), (b) four drops of TfOH (pale yellow), (c) previous sample after some time (bright yellow). Additional signals not seen in neutral spectra of **1a** (**1**) are marked in green.

When comparing the experimental spectra with the data obtained by George E. Salnikov et al.⁵⁶, signal *B* could be assigned to protonated acetamide (Figure 14, **2**). According to the literature, acetamide is likely to be one of the major reaction products as the CH_3CN molar ratio to the TfOH was very high ($\approx 100:1$). The other formed side products are tautomers **3** and **4**. In the solution, these molecules will undergo an electrophilic attack, forming compound **5**, or oligomerisation, producing compound **6** and other higher-ordered oligomers.⁵⁶ These oligomers could be the reason for the changes in the viscosity and colour of the samples in this thesis. Furthermore, changes in the viscosity of the samples could be one of the contributing factors to our inability to quantify dimerisation constants.

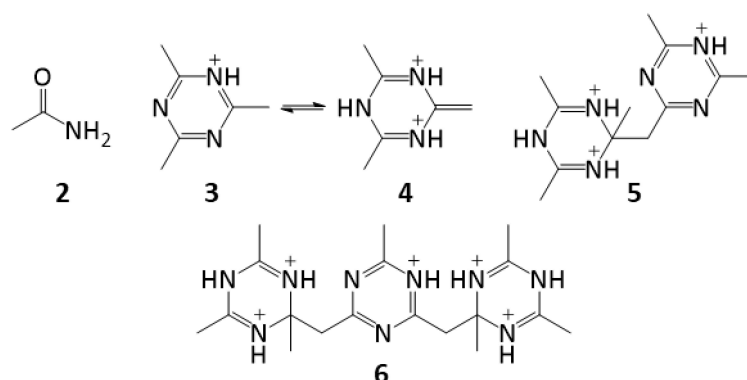


Figure 14. Compounds that are formed in the reaction of CH_3CN and TfOH.⁵⁶

2.2.6. Conclusion of the Experiments with TfOH

In conclusion, the initial experiments with TfOH were promising in finding information about the dimerisation of **1a**. From the first dilution experiment with TfOH, an association of the initial chemical shift changes of the protons in the coumarin moiety to dimerisation of the molecule could be made. However, further calculations of the dimerisation constant could not be performed due to the findings of multiple processes in the experiments and CH_3CN and TfOH reaction products.

Hence, based on our findings, the combination of CH₃CN and TfOH is unsuitable for studying dimerisation between novel phosphazene based fluorophore **1a**.

2.3. Analysis of **1a** in Acidic Conditions with the Addition of HCl

Further experiments to investigate the aggregation of **1a** were conducted using 37 % HCl as an acidifying agent.

2.3.1. Comparison of the Neutral and Protonated **1a** NMR spectra

In the figure below, one can observe the spectrum of experiment 1 (Figure 15a) captured in a neutral environment compared to the spectrum of experiment 6 (Figure 15b) in an acidic environment. Similarly, to experiment 2 with TfOH (Figure 9), the chemical signals of the protonated sample were shifted downfield compared to the signals of the neutral molecule, confirming the protonation of **1a** with HCl in experiment 6.

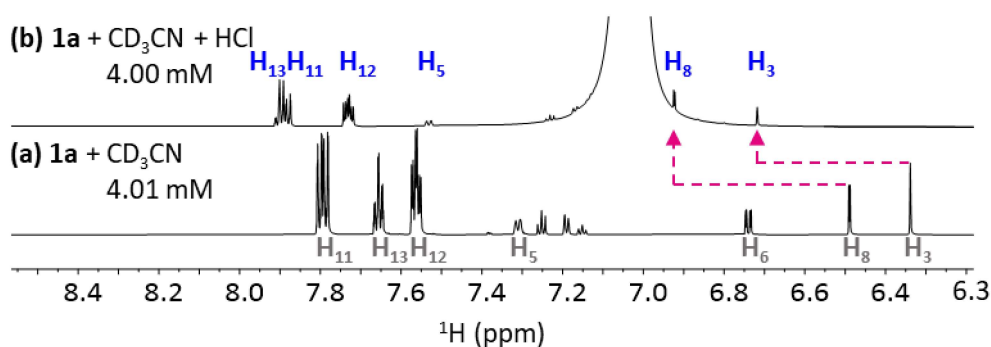


Figure 15. ¹H NMR spectra of **1a** in CD₃CN: (a) of experiment 1 at 4.01 mM spectrum at 298 K, (b) of experiment 6 at 4.00 mM spectrum acidified with a drop of HCl at 298 K. The proton signals of **1a** are marked in grey and **1a*** in blue. Pink arrows indicate signals downfield shifts due to protonation.

2.3.2. Spectral Changes in Experiment 6

Experiment 6 was performed similarly to 2 however, a drop of HCl was used instead of TfOH, then serial dilutions were made, and their ¹H NMR spectra were measured.

In experiment 6 spectra (see Figure 16), the water signal overlapped with the investigated signals, making observations of the chemical shift changes of **1a** signals difficult. Although uniform chemical shift changes were detected for the H₃, H₆ and H₈ (Figure 16), their pattern change, sigmoidal function or S-curve, is more complex and challenging to rationalise than the experiments conducted with TfOH (Figure 10).

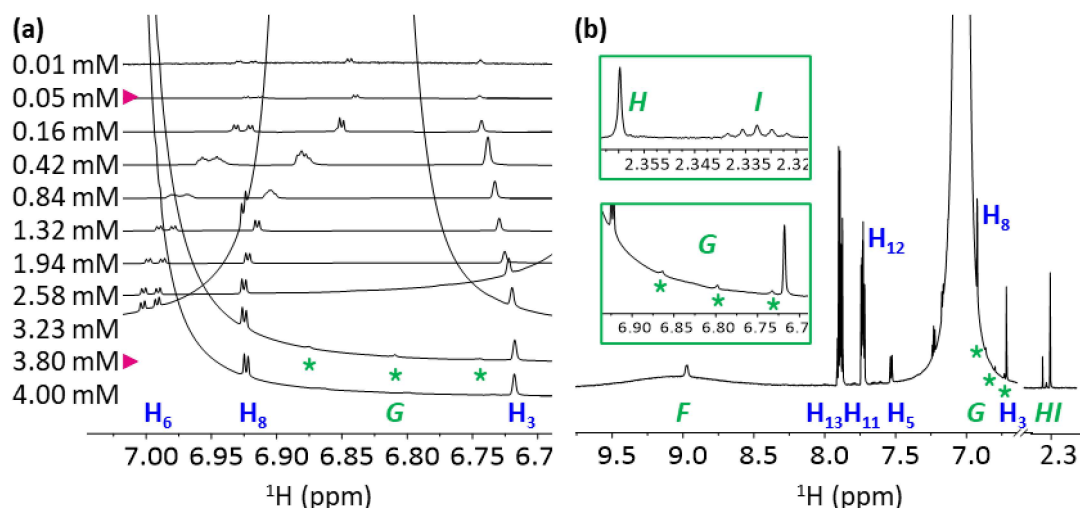


Figure 16. ^1H NMR spectra of experiment 6 of **1a** in CD_3CN acidified with one drop of HCl at 298 K: (a) stacked spectra of the serial dilutions with a zoom to the areas of interest, (b) the full spectrum at 4.00 mM. The proton signals of **1a**^{*} are marked in blue and additional signals not seen in the neutral spectra (**1**) are marked in green.

In the case of experiment 6, we would expect the transition point of the mostly dimer present in the sample to the protonated monomer to be at 3.80 mM. In experiment 2 (Figure 10), it was identified to be at 1.32 mM. The less acidic environment in experiment 6 compared to 2 (see comparative spectra in Appendix 1, Figure 30) explains the earlier dissociation of the dimer to protonated monomer. Here again, one could observe the chemical shift of the water signal to evaluate the acidity of the samples.

Similarly to experiment 2, signals H_6 and H_8 exhibit initial downfield movements upon dilution as dimers dissociate to protonated monomers, followed by upfield shifts due to decreased protonation of the molecules. Opposite shift directions were experienced with H_3 . Interestingly, the H_6 and H_8 signals in the 0.01 mM spectra are slightly more deshielded than the signals in the 0.05 mM spectrum. This shift can occur for various reasons, one of them being reaction products of the HCl and the solvent, which are described later in detail.

2.3.3. Evaluation of the Additional Signals in Experiment 6

When the signals were integrated in the experiment 6 spectra (Figure 16), the overall integration of the proton signals in the aromatic region between 7.84–7.93 ppm (assigned to H_{11} and H_{13}) revealed 10 protons (Appendix 1, Figure 28). The additional proton was previously assigned to H_{14} .

Furthermore, similarly to the TfOH experiments, many additional peaks had appeared (Figure 16). This time singlet (*H*) and pentet (*I*) in the 2.4 ppm, three singlets (*G*) in the 6.8 ppm and signal *F* in the 8.7–9.5 ppm range.

2.3.4. Kinetic Experiment with the Addition of HCl

To investigate if the changes that occurred in the two-photon experiment spectra over time were constant³⁰, kinetic experiment 7 was conducted to study how the sample is changing over a period

of time. For this, 4.00 mM of **1a** solution in CD₃CN was prepared, acidified with one drop of HCl and measured at different time intervals for 21 h.

Figure 17 exhibit the spectra of experiment 7, here, one could observe that the signals belonging to the compound protons (marked in blue) do not have significant chemical shifts nor intensity changes, however, the additional signals *F* and *G* are moving downfield and intensifying. Also, the signal *I* is growing in intensity over the measurement time. This led to the assumption that the additional signals (marked in green) might not be associated with the molecule under investigation but with solvent and acid interaction.

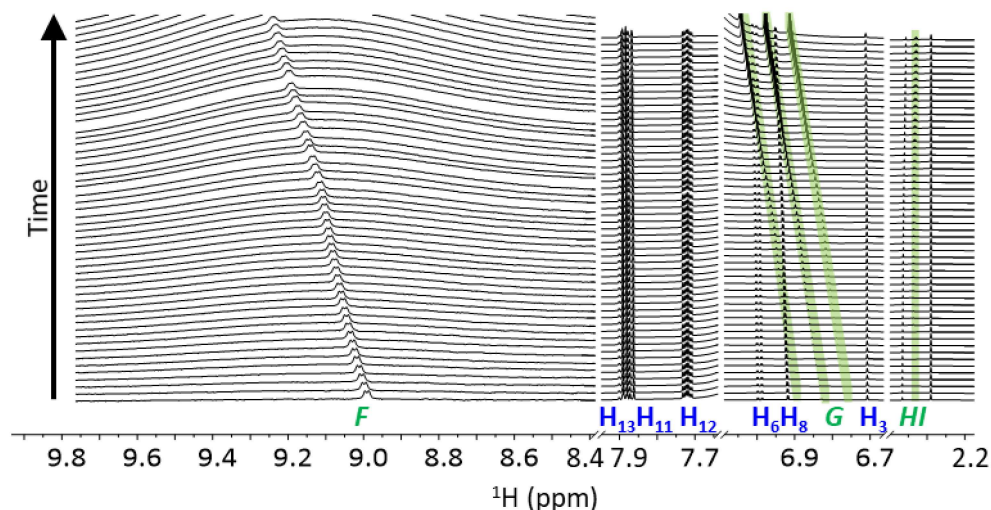


Figure 17. ¹H NMR stacked spectrum of experiment 7 at 4.00 mM **1a** in CD₃CN acidified with one drop of HCl at 298 K with time intervals from 11–1260.5 minutes. The proton signals of **1a**^{*} are marked in blue and additional signals not seen in the neutral spectra (**1**) are marked in green. To illustrate signal *F* intensity changes during time, this part of the spectra has been made more intense compared to the other regions.

2.3.5. Acetonitrile and HCl Interactions

After the kinetic experiment 7 was measured, the sample was left at room temperature, and within five days, colourless crystals (Figure 18a) formed in the NMR tube. At first, there were two distinct layers in the solution, however, they disappeared after a month. Since there was the assumption that additional signals in the spectra appear from the solvent and acid interactions, a drop of HCl was added to pure CD₃CN solvent, which led to the formation of crystals of similar morphology (Figure 18b), supporting the hypothesis. Attempts to resolve the crystal structure of the sediment were unsuccessful.

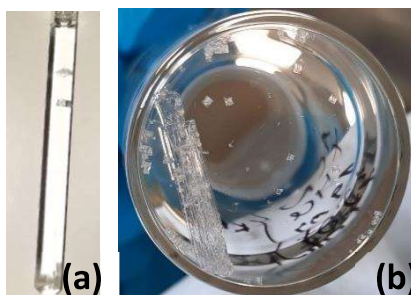


Figure 18. (a) – crystals formed in the kinetic experiment 7 NMR sample after five days. The sample was made of 4.00 mM **1a** in CD₃CN and acidified with HCl. (b) – crystals formed in the CD₃CN acidified with a drop of HCl.

Following this, the hypothesis was made that additional signals *G*, *H*, *I* and *F* from experiment 6 spectra (Figure 16) indicate the presence of acetic acid and ammonium chloride formed from acid-catalysed hydrolysis of nitriles. The triplet signal *G* was assigned to the NH₄⁺ according to literature⁵⁷, where a 1:1:1 triplet was detected in the region of 7.17 ppm with $J_{^{14}\text{N}-^1\text{H}}$ coupling value of 52 Hz. From the Cambridge Isotope Laboratories NMR solvent data chart, the methyl group signal of the acetic acid-*d*₄ was identified as the pentet signal *I* in the 2.33 ppm with the coupling constant of 2.29 Hz.⁵⁸ Broad signal *F* in the 8.8-9.8 ppm range could belong to the acidic proton of acetic acid.

To investigate the appearance of these additional signals in the NMR spectra, a reference sample consisting of CD₃CN with a drop of HCl was measured (Figure 19). The resulting spectra of experiment 8 strengthen the assumption that extra signals that were not seen in the spectra of neutral **1a** (marked in green) were again caused by CH₃CN and acid interactions as it was with TfOH.

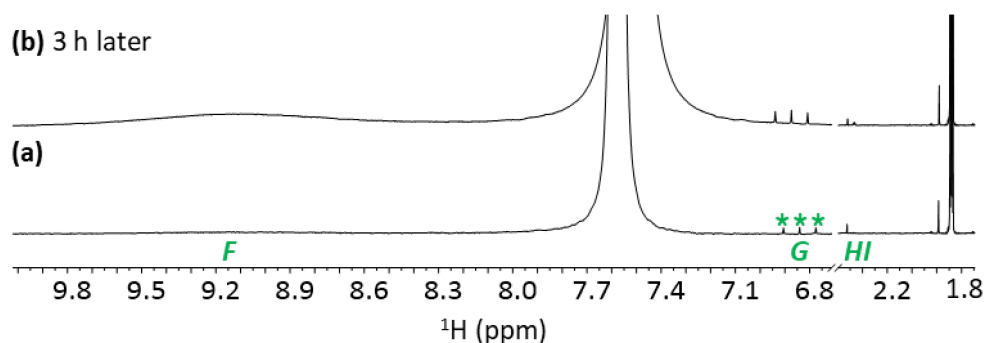


Figure 19. ¹H NMR stacked spectra of experiment 8 of CD₃CN acidified with a drop of HCl at 298 K: (a) spectrum was measured immediately after adding the acid, (b) 3 hours after the acid addition. Additional signals not seen in neutral spectra (1) of **1a** are marked in green.

Comparing the spectra of the samples taken 3 hours apart, one could observe the increase in the intensity for the signals *F*, *G* and *I* (Figure 19b), as was seen in the kinetic experiment 7 spectra (Figure 17).

2.3.6. Conclusion of the Experiments with HCl

In conclusion, the data obtained from the first experiment with HCl indicated the possibility of dimerisation of **1a**. However, discoveries of CD₃CN and HCl reaction products in the NMR spectrum prevent definite assumptions about the dimerisation or aggregation of **1a**, especially when one of

the reaction side products is another acid, which concentration is observed to increase during the kinetic experiment.

3. Experimental

3.1. General Information

All NMR experiments were carried out using Eurisotop CD₃CN as a solvent and Bruker Avance-III-800 MHz spectrometer. Compound **1a** was provided by Matt Rammo and weighted with Sartorius Microbalance with the precision of 1 µg. For the experiments in acidic conditions, trifluoromethanesulfonic acid (TfOH, Sigma-Aldrich, 99 %) and hydrochloric acid (HCl, Sigma-Aldrich, 37 %) were used. Solutions were placed into 3 or 5 mm NMR tubes with Hamilton syringes and homogenised by vortexing the samples.

All the spectra gathered were analysed with MestReNova software. Chemical shifts were referenced based on CD₃CN residual peak (pentet) at 1.940 ppm and processed with baseline and phase corrections. Bindfit⁵³ was used as an example of a data fitting program to calculate the dimerisation constants.

3.2. Experimental Procedures

The dilution experiments 1, 2 and 6 ¹H NMR spectra were collected as soon as the samples were prepared in the order of concentration decrease. Measurements were taken with P1 = 30 °, other parameters for the experiments can be found in the appendix (Appendix 3, Table 4). Experiments taken to investigate **1a** dimerisation are listed in Table 1.

Table 1. Experiment notations and descriptions of ¹H experiments were conducted to investigate coumarin derivative dimerisation.

Experiment notation	Description of conducted ¹ H experiments
1	Dilution experiment with 1a in CD ₃ CN
2	Dilution experiment with 1a in CD ₃ CN acidified with a drop of TfOH
3	Dilution experiment in a constantly acidic environment with 1a in CD ₃ CN acidified with 2.5 µl of TfOH
4	Dilution experiment in a constant acidic environment with 1a in CD ₃ CN acidified with 10 µl of TfOH
5	Interaction between CD ₃ CN and TfOH
6	Dilution experiment with 1a in CD ₃ CN acidified with a drop of 37 % HCl
7	Kinetic experiment with 4 mM 1a in CD ₃ CN acidified with a drop of 37 % HCl
8	Interaction between CD ₃ CN and HCl
9	COSY experiment of 1a

1 – dilution experiment in neutral conditions

The first sample was prepared by dissolving 1.275 mg of coumarin derivative **1a** in 650 µl CD₃CN, 600 µl of the solution was added to a 5 mm NMR tube, and the ¹H NMR spectrum was measured. After measuring the first sample, the solution was pipetted from the NMR tube to a vial. For the second sample, a defined volume (see Appendix 3, Table 5) of the first sample was placed in a new

NMR tube and diluted to a specific concentration with CD₃CN. The dilution series of the samples was conducted according to the dilution method described for sample two.

It was decided to omit samples 7, 8 and 10 from the NMR measurements during the experiment because previous measurements did not show any spectral changes or significant chemical shift changes.

2 and 6 – dilution experiments in acidic conditions

Serial dilutions were conducted in the same manner as in experiment 1 however, before the NMR measurements, a drop of TfOH for experiment 2 and a drop of HCl for experiment 6 were added. This destained the previously yellow solution into colourless. The dilution row was conducted as described before.

3 – dilution experiment with 2.5 µl of TfOH

The stock solution was made by dissolving 6.109 mg of **1a** in 1584.7 µl CD₃CN. The yellow stock solution was added to 3 mm NMR tubes according to the experimental plan (Appendix 3, Table 6) and diluted to a specific concentration with CD₃CN. Before the first measurements, 2.5 µl of TfOH was added to every tube, giving colourless samples.

Dilution series were measured with an autosampler in the consecutive row.

4 - dilution experiment with 10 µl of TfOH

When the spectra of experiment 3 were analysed, the decision was made to add more acid (7.5 µl) to unify the acidity of the samples. After adding the extra TfOH (in total 10 µl) first three samples turned yellow.

5 – CD₃CN and a drop of TfOH, four drops of TfOH and after some time

For the experiment, 150 µl of the CD₃CN and a drop of TfOH were added to the 3 mm NMR tube and measured. After the first measurement, more acid was added (in total, four drops), the solution turned pale-yellow, and the sample was measured. The third measurement was conducted after some time when the sample had turned bright yellow.

7 – kinetic experiment

Experiment 7 was carried out with 1.278 mg of the **1a** in the 600 µl CD₃CN solution acidified with a drop of 37 % HCl. In this experiment, ¹H NMR spectra were measured after different time intervals (Appendix 3, Table 7) to see how the sample changed over time.

8 - CD₃CN and a drop of HCl

Sample preparation and the NMR measurements were conducted in the same manner as in experiment 5, but with HCl. Two spectra were collected: one after adding a drop of acid and the second after 3 hours.

9 – COSY experiment

For the experiment, 0.866 mg of **1a** was dissolved in 600 µl of CD₃CN, and the COSY spectrum was measured.

3.3. Data Fitting with Bindfit

Although Bindfit fits were conducted in this thesis, their data cannot be used as an indicator of self-assembly of **1a** due to the multiple processes in the samples and interactions of acid and solvent.

An excel file was created to fit the chemical shift data obtained from the NMR spectroscopy measurements with Bindfit. The file consisted of molar concentrations (C , M) of the samples, and corresponding chemical shifts (δ , ppm) of the signal under investigation were added. Chemical shifts of the signals were obtained from Mnova. The Bindfit fits in this thesis were undertaken as a learning exercise and are included for completion.

The completed files were uploaded in the Bindfit for NMR dimer aggregation fitting. The method used for data fitting was Nelder-Mead (Simplex), as the program recommended it as a more powerful option. Also, the parameter “Subtract initial values” was unticked to include the first data row into the fitting.

Conclusions

The present research aimed at determination of any possible self-association of the protonated form of the novel phosphazene based pH sensor **1a** with NMR spectroscopy. In the ^1H spectra, shifts of the chemical signals, especially H_3 , H_6 and H_8 , were monitored as an indicator of protonation and dimerisation. According to the literature, the protonation of the nitrogen atom, linking coumarin and phosphazene moiety, causes downfield shifts of the **1a** signals due to diminished conjugation in the aromatic system. The opposite was found for dimerisation, in the dimer conjugation is partially restored as carbonyl oxygen donates its electron density to nitrogen atom via hydrogen bond formation.

This study has shown that:

- Protonation is the key factor for the potential dimerisation of **1a**, as no significant chemical shift changes were observed in the dilution series experiment in neutral conditions.
- Experiments conducted in acidic conditions with TfOH and HCl suggest protonation and dimerisation of the molecule, as the chemical shift changes corresponding to diminished conjugation upon protonation and restored conjugation upon dimerisation were detected.
- Also, the third process corresponding to chemical shift changes indicating deprotonation of the nitrogen atom was seen at higher dilutions.
- The additional signals were discovered and subsequently assigned to acidic hydrolysis reaction products of the acid and solvent. Both acids used in the experiments were reacting with CH_3CN .

Although preliminary findings supported the hypothesis of self-dimerisation of **1a**, the unanticipated discovery of extra signals and the occurrence of the multiple processes in the dilution series made it difficult to quantify dimerisation and, therefore, to calculate respective association constant.

This thesis has provided a deeper insight into the processes that occurred in the solutions investigated by Matt Rammo and co-workers⁴. Based on NMR results, the main question of whether the assumed self-dimerisation is connected to the 1PA and 2PA spectral mismatch remains inconclusive. However, comparison of experimental conditions and underlying assumptions associated with NMR and optical spectroscopy provides a further advantage in assessment of the dimerisation hypothesis. In that respect, both the concentration mismatch (usual concentrations used in optical spectroscopy are below dimerisation threshold determined by NMR) and structural differences (NMR favours bidentate dimers while quantum chemical calculations suggest that low-lying absorption features stem from monodentate dimers) render dimerisation hypothesis unlikely source of the observed absorption properties.

Acknowledgements

I would like to thank my supervisors, Jasper Adamson and Helena Vanessa Roithmeyer. During the year we worked together, I have gained a lot of knowledge, and your trust and support have encouraged me to be more confident and independent. I am incredibly grateful of Helena, who took the time to help me through this process, although you had so much going on for yourself.

In addition, I would like to thank Riina Aav for her support during my studies, for introducing me to NMR and for the help and hints in solving the spectral puzzle in this thesis.

I would also like to show gratitude to Indrek Reile, Kerti Ausmees, Nele Reimets, Vitalijs Rjabovs and others for the help and support you have given me.

I am grateful for the cooperation with Aleksander Rebane and his research group, leading with Matt Rammo, Merle Uudsemaa and Aleksander Trummal.

I have been fortunate to work and study with such amazing people in NICPB and TalTech.

References

- (1) McDonagh, C.; Burke, C. S.; Maccraith, B. D. Optical Chemical Sensors. *Chemical Reviews* **2008**, *108* (2), 400–422. <https://doi.org/10.1021/cr068102g>.
- (2) Wencel, D.; Abel, T.; McDonagh, C. Optical Chemical PH Sensors. *Analytical Chemistry* **2014**, *86* (1), 15–29. <https://doi.org/10.1021/ac4035168>.
- (3) Selberg, S.; Pagano, T.; Tshepelevitsh, S.; Haljasorg, T.; Vahur, S.; Luik, J.; Saame, J.; Leito, I. Synthesis and Photophysics of a Series of Lipophilic Phosphazene-Based Fluorescent Indicators. *Journal of Physical Organic Chemistry* **2019**, *32* (7). <https://doi.org/10.1002/poc.3950>.
- (4) Rammo, M.; Trummal, A.; Uudsemaa, M.; Pahapill, J.; Petritsenko, K.; Sildoja, M.; Stark, C. W.; Selberg, S.; Leito, I.; Palmi, K.; Adamson, J.; Rebane, A. Novel Lipophilic Fluorophores with Highly Acidity-Dependent Two-Photon Response. *Chemistry – A European Journal* **2022**, *28* (8). <https://doi.org/10.1002/chem.202103707>.
- (5) Selberg, S. Synthesis and Properties of Lipophilic Phosphazene-Based Indicator Molecules. Doctoral Thesis, Tartu Ülikool, Tartu, 2019.
- (6) Marczewska, B.; Marczewski, K. First Glass Electrode and Its Creators F. Haber and Z. Klemensiewicz – On 100th Anniversary. *Zeitschrift für Physikalische Chemie* **2010**, *224* (5), 795–799. <https://doi.org/10.1524/ZPCH.2010.5505/MACHINEREADABLECITATION/RIS>.
- (7) Sun, X.-Y.; Liu, T.; Sun, J.; Wang, X.-J. Synthesis and Application of Coumarin Fluorescence Probes. *RSC Advances* **2020**, *10* (18), 10826–10847. <https://doi.org/10.1039/c9ra10290f>.
- (8) Wencel, D.; Kaworek, A.; Abel, T.; Efremov, V.; Bradford, A.; Carthy, D.; Coady, G.; McMorro, R. C. N.; McDonagh, C. Optical Sensor for Real-Time PH Monitoring in Human Tissue. *Small* **2018**, *14* (51). <https://doi.org/10.1002/smll.201803627>.
- (9) Wolfbeis, O. S. *Fiber Optic Chemical Sensors and Biosensors*; CRC Press: Boca Raton, 1991; Vol. 1.
- (10) Cammann, G. G.; Guilbault, E. A.; Hal, H.; Kellner, R.; Wolfbeis, O. The Cambridge Definition of Chemical Sensors. In *Cambridge Workshop on Chemical Sensors and Biosensors*; Cambridge University Press: New York, 1996.
- (11) Schwesinger, R.; Schlemper, H.; Hasenfratz, C.; Willaredt, J.; Dambacher, T.; Breuer, T.; Ottaway, C.; Fletschinger, M.; Boele, J.; Fritz, H.; Putzas, D.; Rotter, H. W.; Bordwell, F. G.; Satish, A. v.; Ji, G. Z.; Peters, E. M.; Peters, K.; von Schnering, H. G.; Walz, L. Extremely Strong, Uncharged Auxiliary Bases; Monomeric and Polymer-Supported Polyaminophosphazenes (P2–P5). *Liebigs Annalen* **1996**, *1996* (7), 1055–1081. <https://doi.org/10.1002/JLAC.199619960705>.
- (12) Klein, D. *Organic Chemistry*, 2nd ed.; Wiley: Hoboken, NJ, 2015.
- (13) Venugopala, K. N.; Rashmi, V.; Odhav, B. Review on Natural Coumarin Lead Compounds for Their Pharmacological Activity. *BioMed Research International* **2013**, *2013*. <https://doi.org/10.1155/2013/963248>.
- (14) Vogel, A. Darstellung von Benzoesäure Aus Der Tonka-Bohne Und Aus Den Meliloten-Oder Steinklee-Blumen. *annalen der physik* **1820**, *64* (2), 161–166.
- (15) Stefanachi, A.; Leonetti, F.; Pisani, L.; Catto, M.; Carotti, A. Coumarin: A Natural, Privileged and Versatile Scaffold for Bioactive Compounds. *Molecules* **2018**, *23* (2), 250. <https://doi.org/10.3390/molecules23020250>.
- (16) Abernethy, J. L. The Historical and Current Interest in Coumarin. *Journal of Chemical Education* **1969**, *46* (9), 561. <https://doi.org/10.1021/ed046p561>.
- (17) Perkin, W. H. VI. - On the Artificial Production of Coumarin and Formation of Its Homologues. *J Chem Soc* **1868**, *21* (63), 53–63. <https://doi.org/https://doi.org/10.1039/JS8682100053>.
- (18) Medina, F. G.; Marrero, J. G.; Macías-Alonso, M.; González, M. C.; Córdova-Guerrero, I.; Teissier García, A. G.; Osegueda-Robles, S. Coumarin Heterocyclic Derivatives: Chemical Synthesis

- and Biological Activity. *Natural Product Reports* **2015**, 32 (10), 1472–1507. <https://doi.org/10.1039/c4np00162a>.
- (19) Mondal, A.; Nag, S.; Banerjee, P. Coumarin Functionalized Molecular Scaffolds for the Effectual Detection of Hazardous Fluoride and Cyanide. *Dalton Transactions* **2021**, 50 (2), 429–451. <https://doi.org/10.1039/d0dt03451g>.
- (20) Lee, K.-S.; Kim, H.-J.; Kim, G.-H.; Shin, I.; Hong, J.-I. Fluorescent Chemodosimeter for Selective Detection of Cyanide in Water. *Organic Letters* **2008**, 10 (1), 49–51. <https://doi.org/10.1021/ol7025763>.
- (21) Vasylevska, A. S.; Karasyov, A. A.; Borisov, S. M.; Krause, C. Novel Coumarin-Based Fluorescent PH Indicators, Probes and Membranes Covering a Broad PH Range. *Analytical and Bioanalytical Chemistry* **2007**, 387 (6), 2131–2141. <https://doi.org/10.1007/s00216-006-1061-6>.
- (22) Duong, H. D.; Shin, Y.; Rhee, J. il. Development of Novel Optical PH Sensors Based on Coumarin 6 and Nile Blue A Encapsulated in Resin Particles and Specific Support Materials. *Materials Science and Engineering C* **2020**, 107. <https://doi.org/10.1016/J.MSEC.2019.110323>.
- (23) Xu, Y.; Jiang, Z.; Xiao, Y.; Zhang, T. T.; Miao, J. Y.; Zhao, B. X. A New Fluorescent Turn-on Chemodosimeter for Mercury Ions in Solution and Its Application in Cells and Organisms. *Analytica Chimica Acta* **2014**, 807, 126–134. <https://doi.org/10.1016/J.ACA.2013.11.042>.
- (24) Yeh, J.-T.; Chen, W.-C.; Liu, S.-R.; Wu, S.-P. A Coumarin-Based Sensitive and Selective fluorescent Sensor for Copper(II) Ions[†]. *New Journal of Chemistry* **2014**, 38 (9), 4434. <https://doi.org/10.1039/c4nj00695j>.
- (25) Gupta, V. K.; Mergu, N.; Kumawat, L. K.; Singh, A. K. Selective Naked-Eye Detection of Magnesium (II) Ions Using a Coumarin-Derived Fluorescent Probe. *Sensors and Actuators, B: Chemical* **2015**, 207 (Part A), 216–223. <https://doi.org/10.1016/J.SNB.2014.10.044>.
- (26) Mizukami, S.; Okada, S.; Kimura, S.; Kikuchi, K. Design and Synthesis of Coumarin-Based Zn 2+ Probes for Ratiometric Fluorescence Imaging. *Inorganic Chemistry* **2009**, 48 (16), 7630–7638. <https://doi.org/10.1021/ic900247r>.
- (27) Helmchen, F.; Denk, W. Deep Tissue Two-Photon Microscopy. *Nat Methods* **2005**, 2 (12), 932–940. <https://doi.org/10.1038/NMETH818>.
- (28) Rammo, M.; Trummel, A.; Uudsemaa, M.; Pahapill, J.; Petritsenko, K.; Sildoja, M.-M.; Stark, C.; Selberg, S.; Leito, I.; Rebane, A. Novel PH-Responsive Highly Fluorescent Lipophilic Coumarins as Efficient Two-Photon Sensors of Acidic and Basic Environments; SPIE-Intl Soc Optical Eng, 2021; p 48. <https://doi.org/10.1117/12.2584084>.
- (29) Rebane, A.; Makarov, N. S.; Drobizhev, M.; Spangler, B.; Tarter, E. S.; Reeves, B. D.; Spangler, C. W.; Meng, F.; Suo, Z. Quantitative Prediction of Two-Photon Absorption Cross Section Based on Linear Spectroscopic Properties [†]. *The Journal of Physical chemistry C* **2008**, 112 (21), 7997–8004. <https://doi.org/10.1021/jp800104q>.
- (30) Rabenstein, D. L. Peer Reviewed: NMR Spectroscopy: Past and Present. *Analytical Chemistry* **2001**, 73 (7), 214–223. <https://doi.org/https://doi.org/10.1021/ac012435q>.
- (31) Becker, E. D. A Brief History of Nuclear Magnetic Resonance. *Analytical Chemistry* **1993**, 65 (6), 295–302. <https://doi.org/https://doi.org/10.1021/ac00054a716>.
- (32) Boesch, C. Nobel Prizes for Nuclear Magnetic Resonance: 2003 and Historical Perspectives. *Journal of Magnetic Resonance Imaging* **2004**, 20 (2), 177–179. <https://doi.org/10.1002/jmri.20120>.
- (33) Maheswaramma, K. S.; Chugh, M. *Engineering Chemistry*, 1th ed.; Pearson Education India: New Delhi, 2016.
- (34) Claridge, T. D. W. *High-Resolution NMR Techniques in Organic Chemistry*, 2nd ed.; Elsevier Science, 2008; Vol. 27.
- (35) Carey, F. A.; Giuliano, R. M.; Allison, N. T.; Bane, S. L. *Organic Chemistry*, 11th ed.; McGraw-Hill Education: New York, 2019.
- (36) Skoog, D. A.; Holler, F. J.; Crouch, S. R. *Principles of Instrumental Analysis*, 7th ed.; Saunders College Pub: Philadelphia, 1998.

- (37) García, J.; Martins, L. G.; Pons, M. NMR Spectroscopy in Solution. In *Supramolecular Chemistry: From Molecules to Nanomaterials*; John Wiley & Sons, Ltd, 2012. <https://doi.org/10.1002/9780470661345.smc019>.
- (38) Kolesnichenko, I. v.; Anslyn, E. v. Practical Applications of Supramolecular Chemistry. *Chemical Society Reviews* **2017**, 46 (9), 2385–2390. <https://doi.org/10.1039/C7CS00078B>.
- (39) Chen, Z.; Weber, S. G. Determination of Binding Constants by Affinity Capillary Electrophoresis, Electrospray Ionization Mass Spectrometry and Phase-Distribution Methods. *Trends in analytical chemistry* **2008**, 27 (9), 738–748. <https://doi.org/10.1016/J.TRAC.2008.06.008>.
- (40) Cowart, A. An Investigation of Noncovalently Bound Supramolecular Systems through Case Studies of Oxacalixarenes and Iodo-Triazoles. Doctoral Thesis, Tallinn University of Technology, Tallinn, 2021. <https://doi.org/https://doi.org/10.23658/taltech.18/2021>.
- (41) Steed, J. W.; Atwood, J. L. *Supramolecular Chemistry*, 2nd ed.; John Wiley & Sons, Ltd, 2009. <https://doi.org/10.1002/9780470740880>.
- (42) Lehn, J.-M. Cryptates: The Chemistry of Macropolycyclic Inclusion Complexes. *Accounts of Chemical Research* **1978**, 11 (2), 49–57. <https://doi.org/10.1021/AR50122A001>.
- (43) Varshey, D. B.; Sander, J. R. G.; Friščić, T.; MacGillivray, L. R. Supramolecular Interactions. In *Supramolecular Chemistry: From Molecules to Nanomaterials*; John Wiley & Sons, Ltd, 2012. <https://doi.org/10.1002/9780470661345.smc003>.
- (44) Socha, O.; Dračínský, M. Dimerization of Acetic Acid in the Gas Phase—NMR Experiments and Quantum-Chemical Calculations. *Molecules* **2020**, 25 (9), 2150. <https://doi.org/10.3390/molecules25092150>.
- (45) Chen, J.-S.; Shirts, R. B. Iterative Determination of the NMR Monomer Shift and Dimerization Constant in a Self-Associating System. *The Journal of Physical Chemistry* **1985**, 89 (9), 1643–1646. <https://doi.org/10.1021/j100255a018>.
- (46) Konrad, N.; Horetski, M.; Sihtmäe, M.; Truong, K.-N.; Osadchuk, I.; Burankova, T.; Kielmann, M.; Adamson, J.; Kahru, A.; Rissanen, K.; Senge, M. O.; Borovkov, V.; Aav, R.; Kananovich, D. Thiourea Organocatalysts as Emerging Chiral Pollutants: En Route to Porphyrin-Based (Chir)Optical Sensing. *Chemosensors* **2021**, 9 (10), 278. <https://doi.org/10.3390/chemosensors9100278>.
- (47) Lehnher, D.; Ford, D. D.; Bendelsmith, A. J.; Kennedy, C. R.; Jacobsen, E. N. Conformational Control of Chiral Amido-Thiourea Catalysts Enables Improved Activity and Enantioselectivity. *Organic Letters* **2016**, 18 (13), 3214–3217. <https://doi.org/10.1021/acs.orglett.6b01435>.
- (48) Wash, P. L.; Maverick, E.; Chiefari, J.; Lightner, D. A. Acid-Amide Intermolecular Hydrogen Bonding. *J Am Chem Soc* **1997**, 119 (16), 3802–3806.
- (49) Hirose, K. A Practical Guide for the Determination of Binding Constants *. *Journal of Inclusion Phenomena and Macrocyclic Chemistry* **2001**, 39, 193–209. <https://doi.org/https://doi.org/10.1023/A:101117412693>.
- (50) Nogales, D. F.; Ma, J.-S.; Lightner, D. A. Self-Association of Dipyrinones Observed by 2D-NOE NMR and Dimerization Constants Calculated from ¹H-NMR Chemical Shifts. *Tetrahedron* **1992**, 49 (12), 2361–2371.
- (51) Thordarson, P. *supramolecular.org*. Bindfit. <http://app.supramolecular.org/bindfit/> (accessed 2022-03-09).
- (52) Hibbert, D. B.; Thordarson, P. The Death of the Job Plot, Transparency, Open Science and Online Tools, Uncertainty Estimation Methods and Other Developments in Supramolecular Chemistry Data Analysis †. *Chemical Communications* **2016**, 52 (87), 12792–12805. <https://doi.org/10.1039/c6cc03888c>.
- (53) Oziminski, W. P.; Dobrowolski, J. C. σ - and π -Electron Contributions to the Substituent Effect: Natural Population Analysis. *Journal of Physical Organic Chemistry* **2009**, 22 (8), 769–778. <https://doi.org/10.1002/poc.1530>.
- (54) Salnikov, G. E.; Genaev, A. M.; Vasiliev, V. G.; Shubin, V. G. Interaction of Acetonitrile with Trifluoromethanesulfonic Acid: Unexpected Formation of a Wide Variety of Structures.

- Organic and Biomolecular Chemistry* **2012**, *10* (11), 2282–2288.
<https://doi.org/10.1039/c2ob06841a>.
- (55) Nielander, A. C.; McEnaney, J. M.; Schwalbe, J. A.; Baker, J. G.; Blair, S. J.; Wang, L.; Pelton, J. G.; Andersen, S. Z.; Enemark-Rasmussen, K.; Čolić, V.; Yang, S.; Bent, S. F.; Cargnello, M.; Kibsgaard, J.; Vesborg, P. C. K.; Chorkendorff, I.; Jaramillo, T. F. A Versatile Method for Ammonia Detection in a Range of Relevant Electrolytes via Direct Nuclear Magnetic Resonance Techniques. *ACS Catalysis* **2019**, *9* (7), 5797–5802.
<https://doi.org/10.1021/acscatal.9b00358>.
- (56) Cambridge Isotope Laboratories, Inc. *NMR Solvent Data Chart*.
https://www.isotope.com/userfiles/files/assetLibrary/NMR_solvents_data_chart_&_storage.pdf (accessed 2022-03-21).

Appendix

Appendix 1. ^1H NMR data, Spectra and Graphs

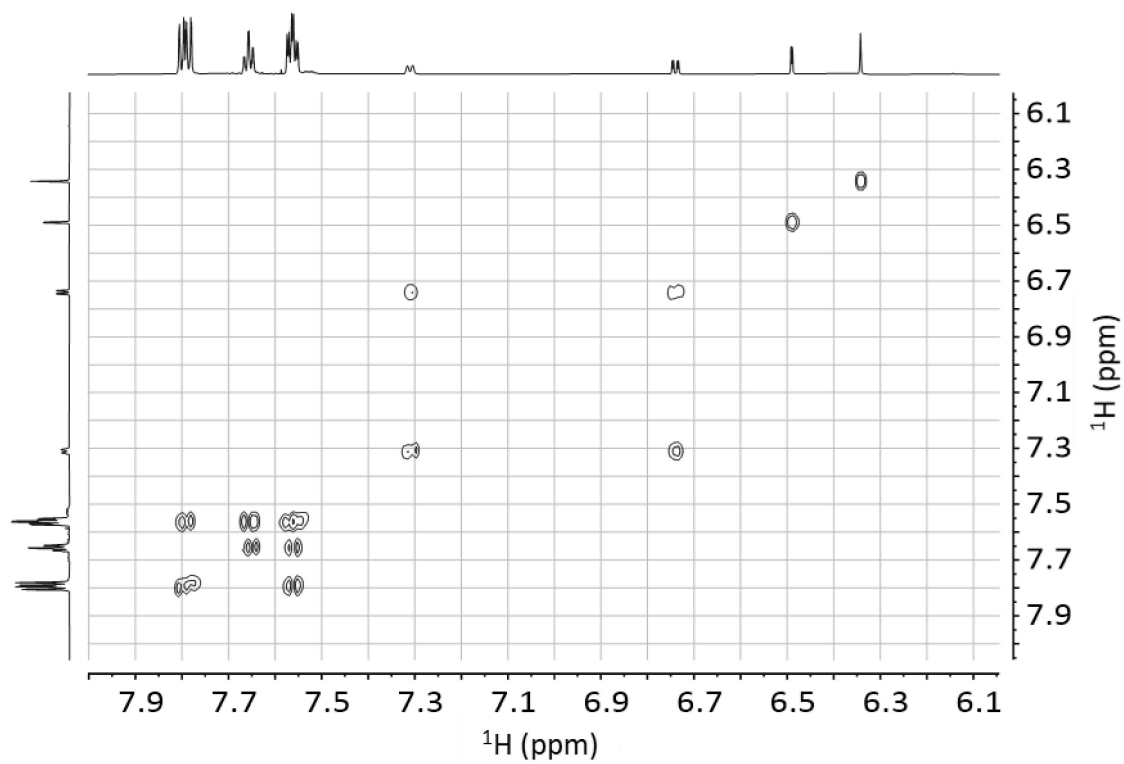


Figure 20. Experiment 9 COSY NMR spectrum of **1a** in CD_3CN at 298 K.

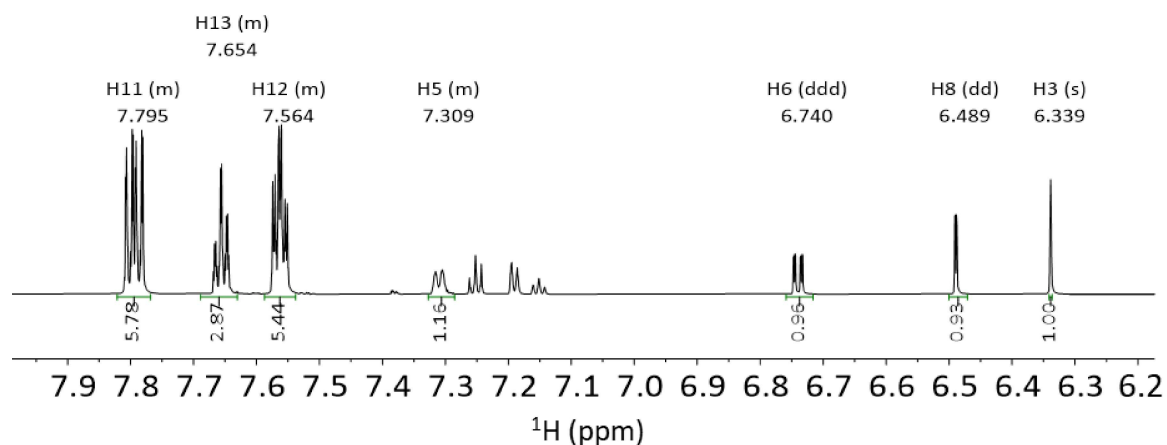


Figure 21. ¹H NMR spectrum of experiment 1 at 4.01 mM **1a** in CD₃CN at 298 K. ¹H NMR (800 MHz, CD₃CN) δ 7.821 – 7.768 (m, 6H), 7.689 – 7.630 (m, 3H), 7.587 – 7.538 (m, 5H), 7.327 – 7.285 (m, 1H), 6.740 (ddd, *J* = 8.9, 2.3, 0.7 Hz, 1H), 6.489 (dd, *J* = 2.2, 0.7 Hz, 1H), 6.339 (s, 1H).

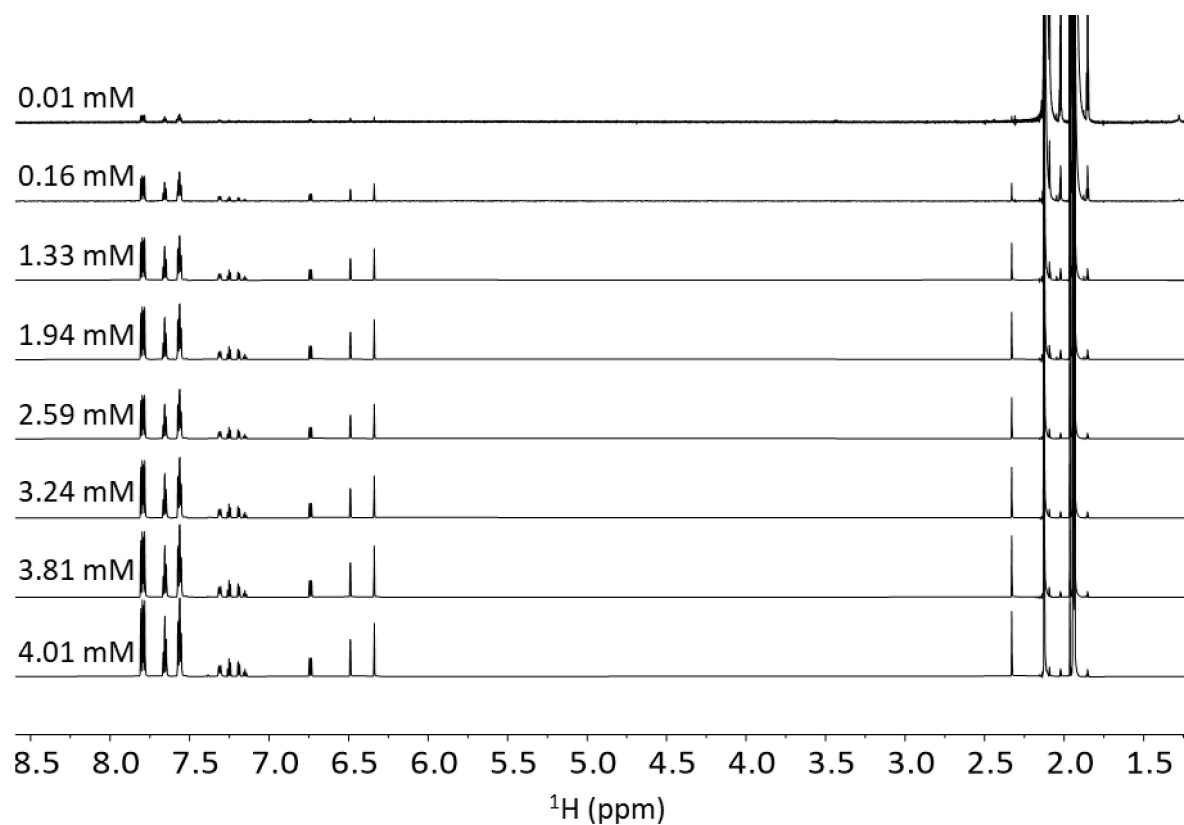


Figure 22. ¹H NMR stacked spectra of the serial dilutions of experiment 1 of **1a** in CD₃CN at 298 K.

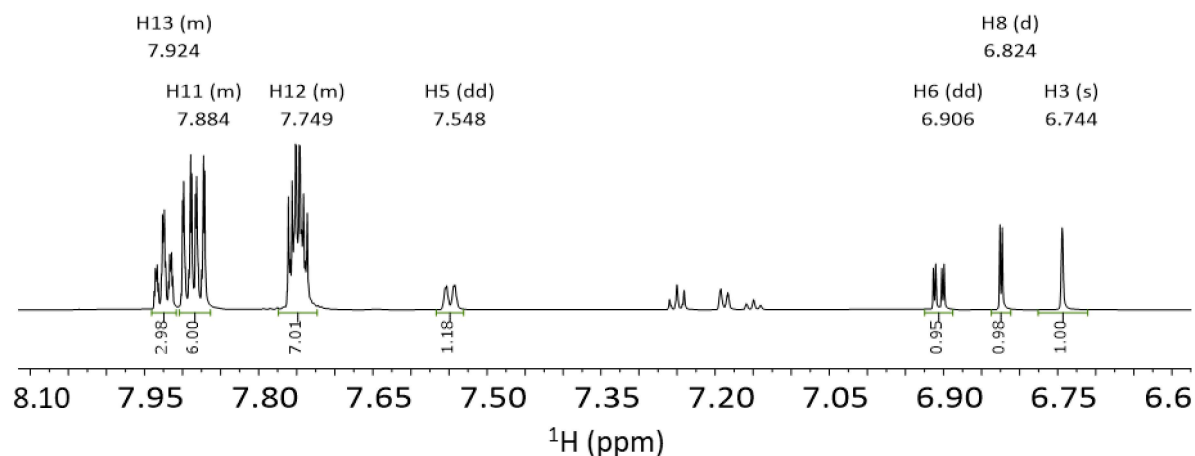


Figure 23. ¹H NMR spectrum of experiment 2 at 4.00 mM **1a** in CD₃CN acidified with one drop of TfOH at 293 K. ¹H NMR (800 MHz, CD₃CN) δ 7.941 – 7.908 (m, 3H), 7.904 – 7.863 (m, 6H), 7.774 – 7.723 (m, 7H), 7.548 (dd, *J* = 8.8, 1.8 Hz, 1H), 6.906 (dd, *J* = 8.9, 2.4 Hz, 1H), 6.824 (d, *J* = 2.4 Hz, 1H), 6.744 (s, 1H).

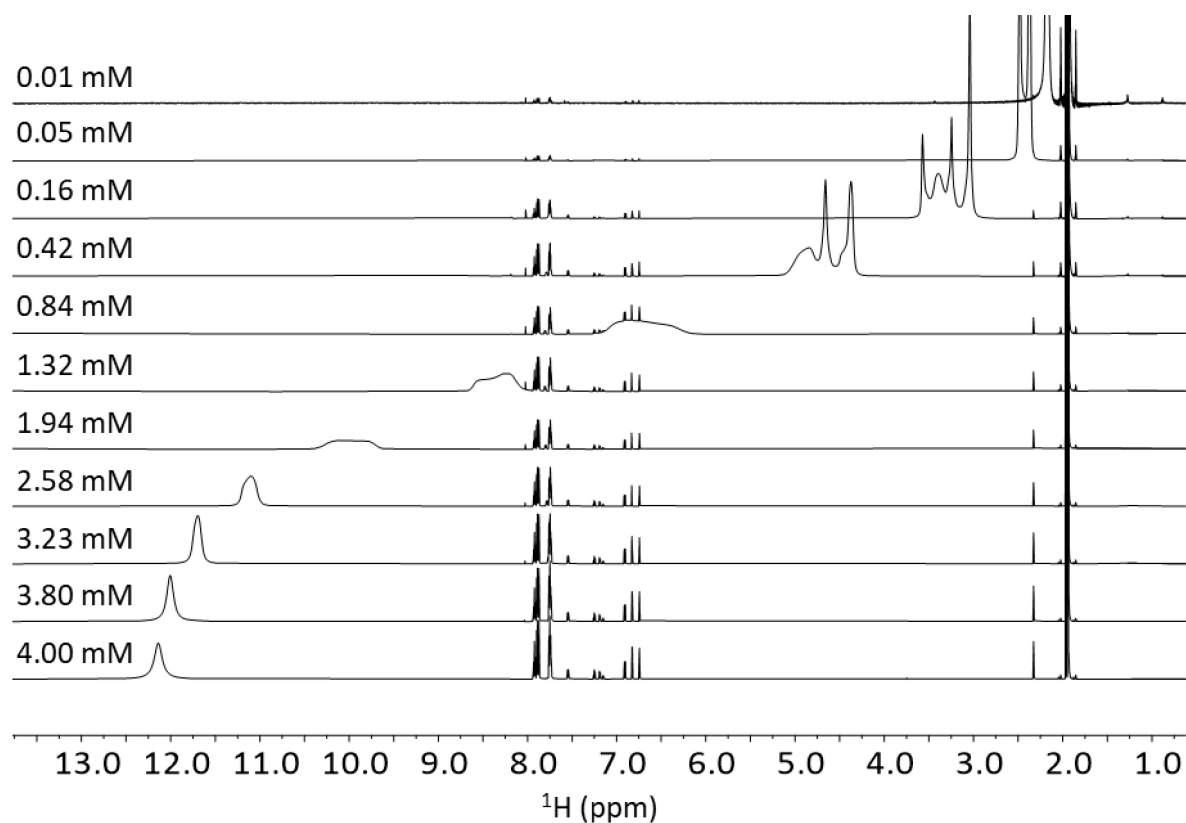


Figure 24. ¹H NMR stacked spectra of the serial dilutions of experiment 2 of **1a** in CD₃CN acidified with one drop of TfOH at 293 K.

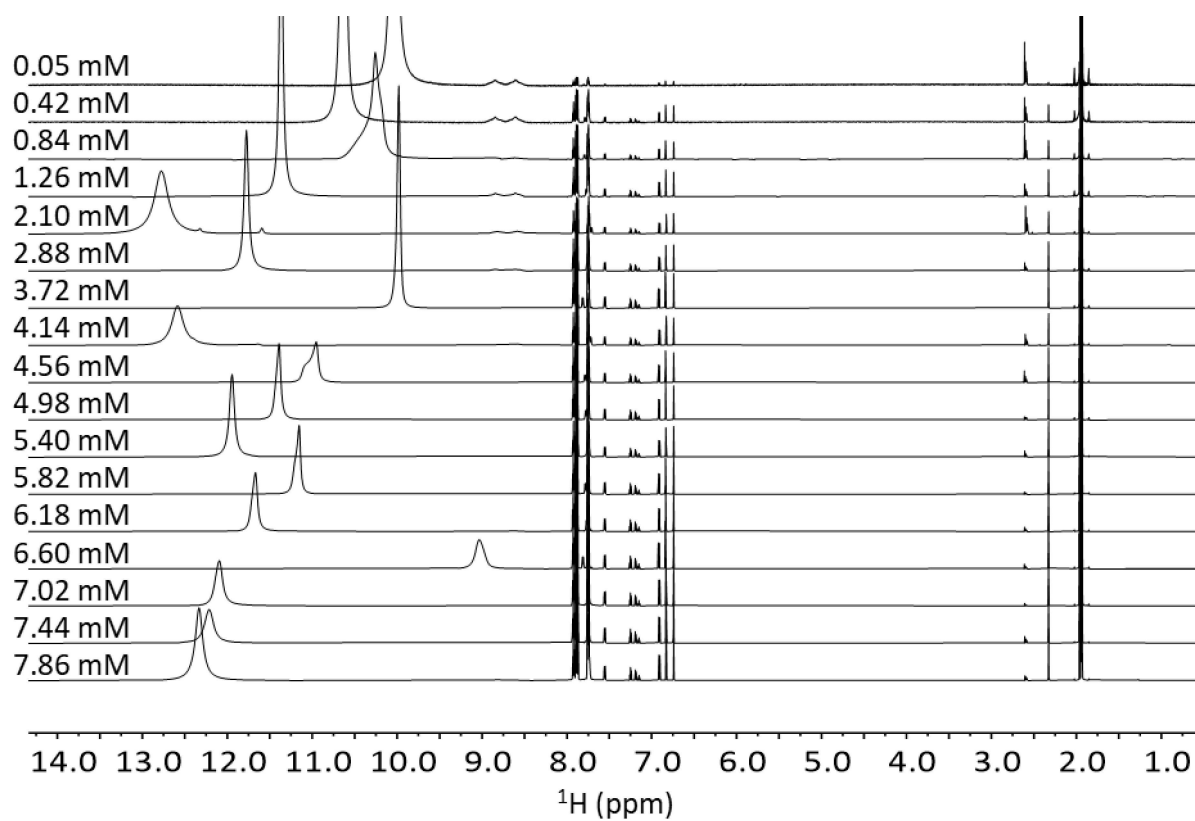


Figure 25. ¹H NMR stacked spectra of the serial dilutions of experiment 4 of **1a** in CD₃CN acidified with 2.5 μl of TfOH at 298 K.

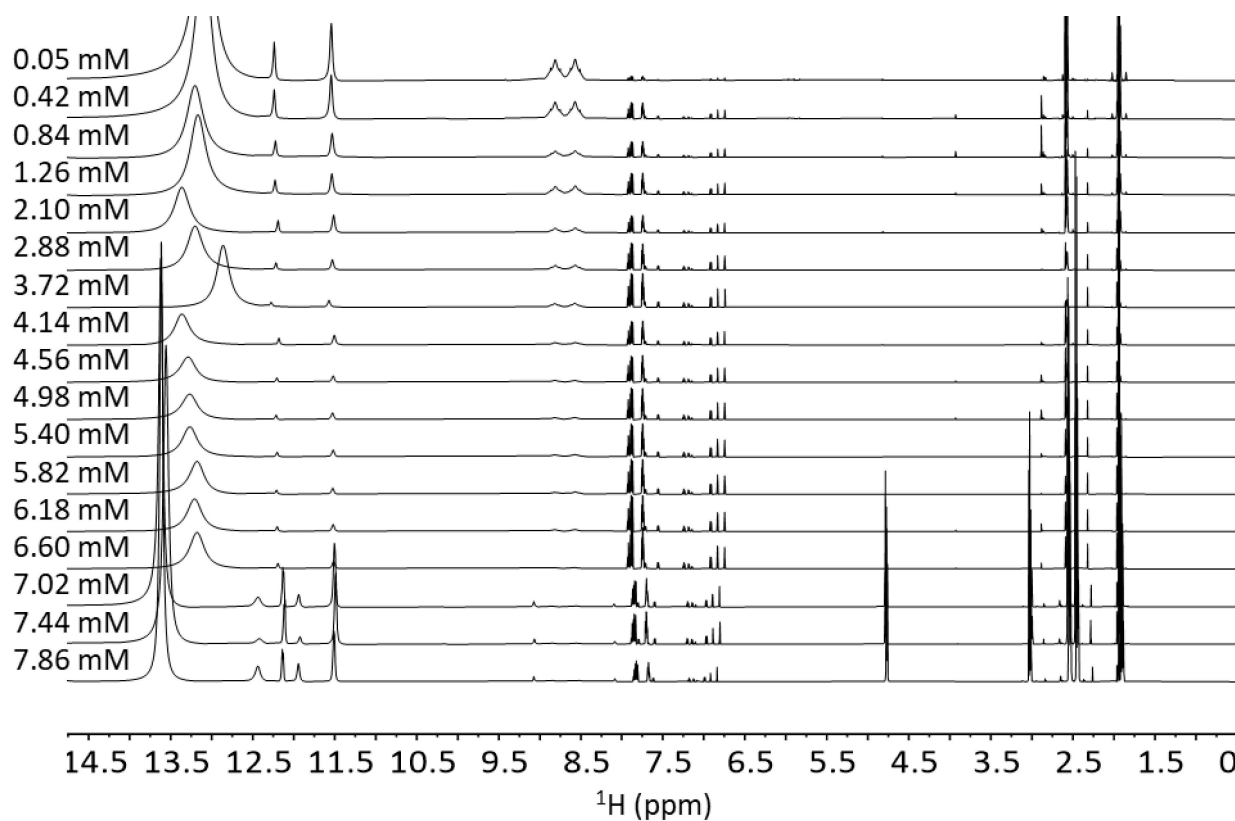


Figure 26. ^1H NMR stacked spectra of the serial dilutions of experiment 4 of **1a** in CD_3CN acidified with $10\ \mu\text{l}$ of TfOH at 298 K.

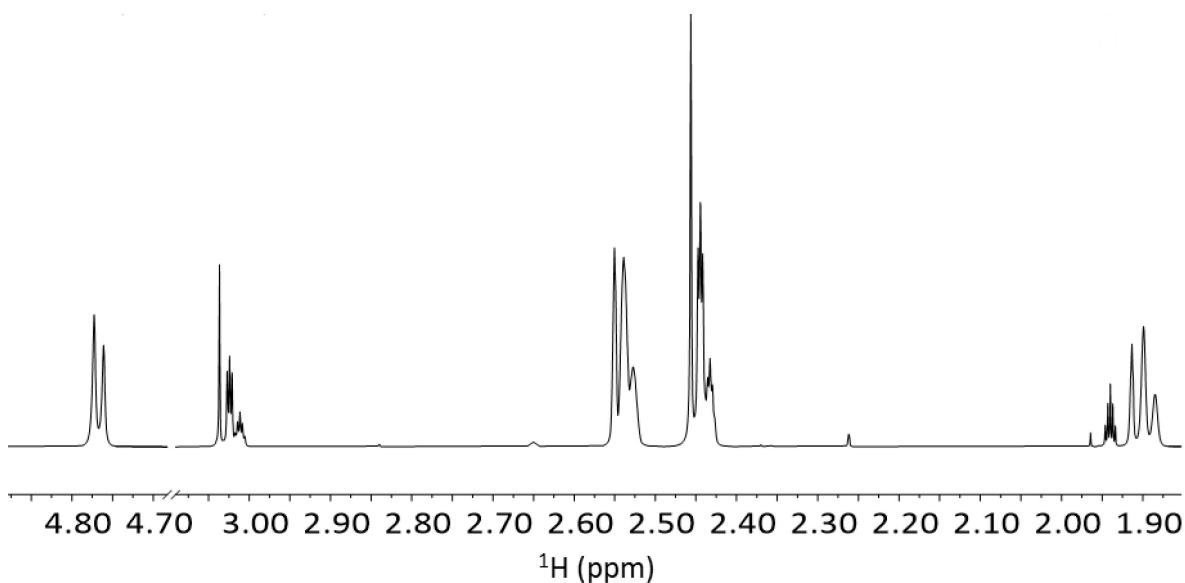


Figure 27. ^1H NMR spectrum of experiment 4 at 7.86 mM **1a** in CD_3CN acidified with $10\ \mu\text{l}$ of TfOH with a zoom to the area of signals *E* at 298 K.

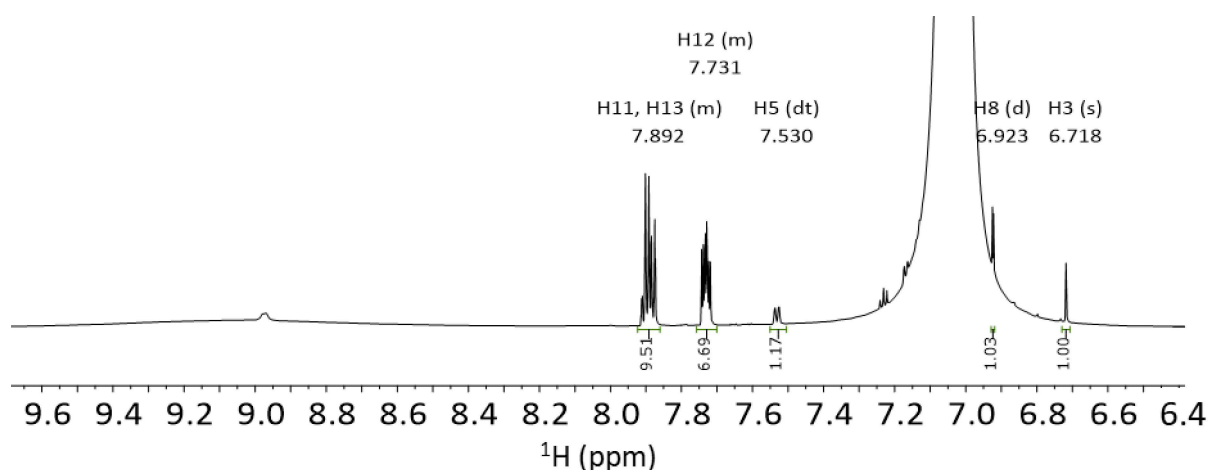


Figure 28. ^1H NMR spectrum of experiment 6 at 4.00 mM **1a** in CD_3CN acidified with one drop of HCl at 298 K. ^1H NMR (800 MHz, CD_3CN) δ 7.923 – 7.860 (m, 10H), 7.757 – 7.700 (m, 7H), 7.530 (dt, $J = 8.9, 2.0$ Hz, 1H), 6.923 (d, $J = 2.4$ Hz, 1H), 6.718 (s, 1H).

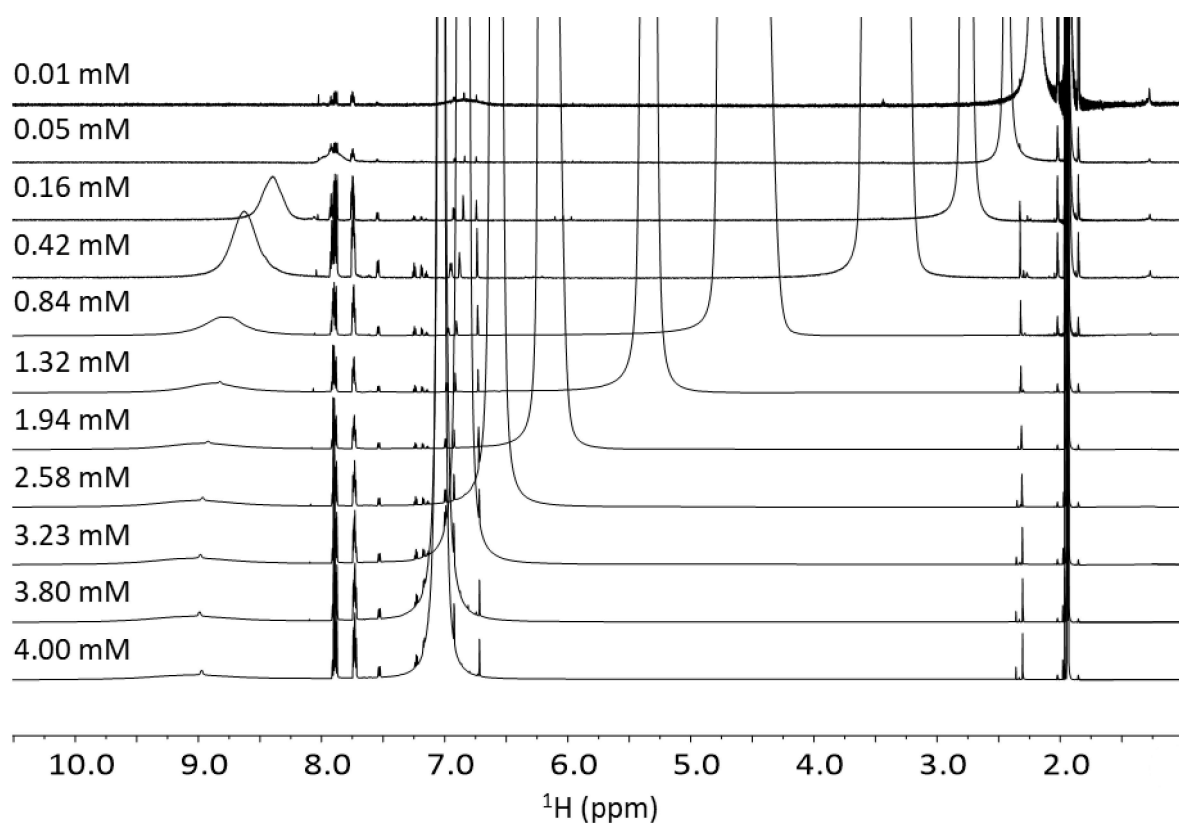


Figure 29. ^1H NMR stacked spectra of the serial dilutions of experiment 6 of **1a** in CD_3CN acidified with one drop of HCl at 298 K.

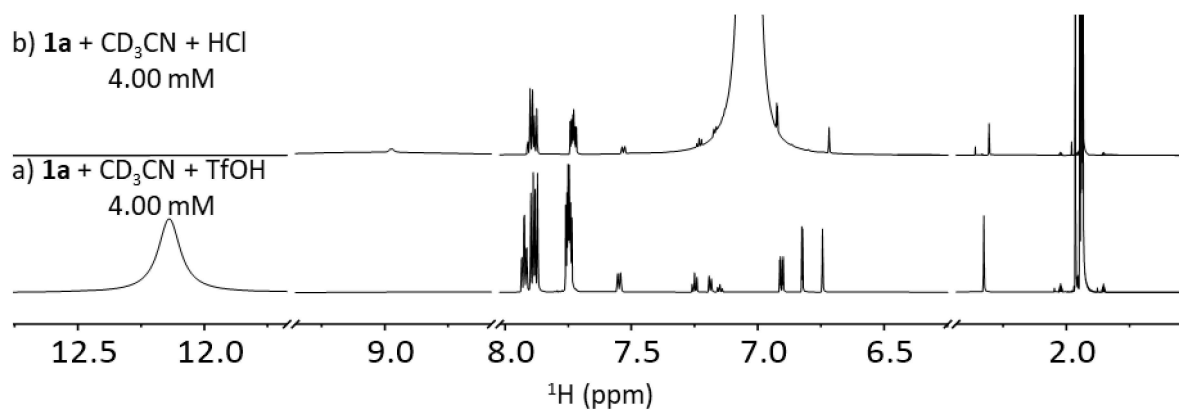


Figure 30. ¹H NMR spectra of **1a** in CD₃CN: (a) of experiment 2 at 4.00 mM spectrum where the sample was acidified with one drop of TfOH at 293 K, (b) of experiment 6 at 4.00 mM spectrum where the sample was acidified with one drop of HCl at 293 K.

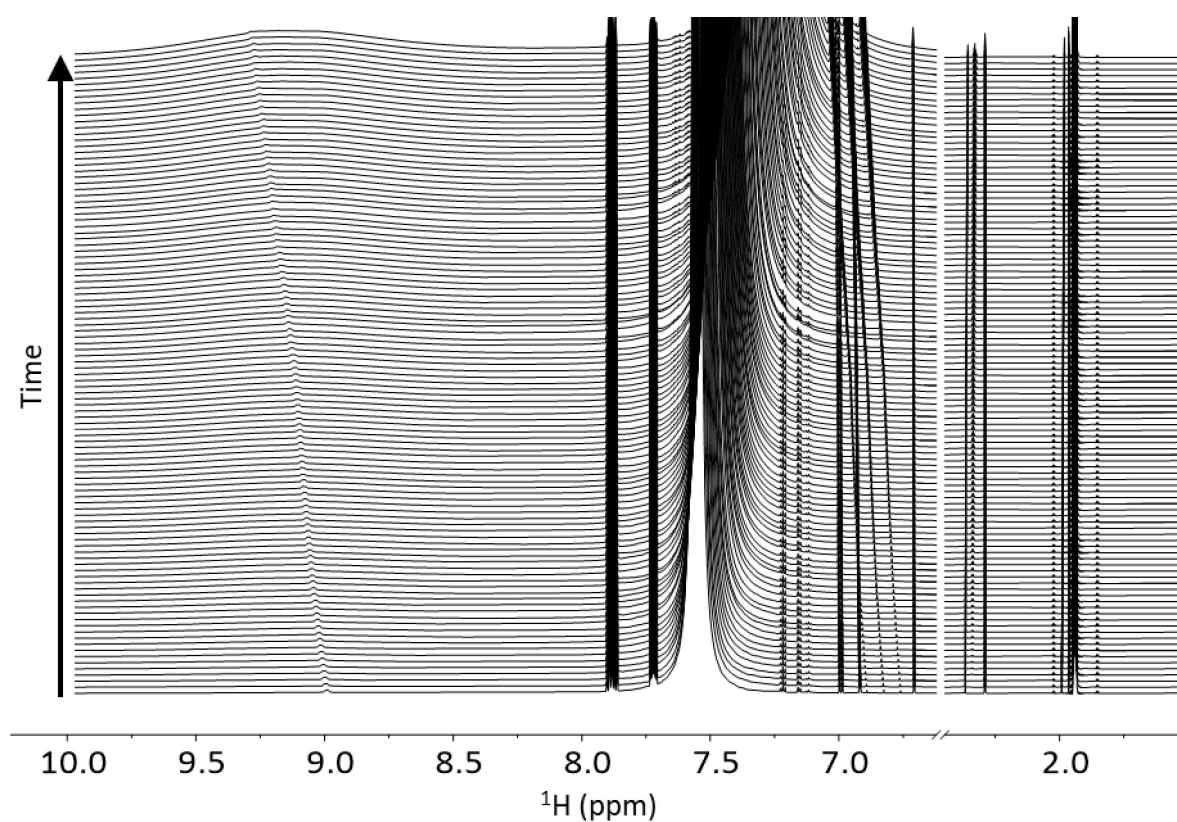


Figure 31. ¹H NMR stacked spectra of experiment 7 at 4.00 mM **1a** in CD₃CN acidified with one drop of HCl at 298 K with time intervals from 11 to 1260.5 minutes.

Table 2. Chemical shifts of the three **1a** signals of interest in the conducted NMR experiments.

Concentration (mM)	Chemical shift (ppm)								
	Experiment 1			Experiment 2			Experiment 6		
	H ₃	H ₈	H ₆	H ₃	H ₈	H ₆	H ₃	H ₈	H ₆
4.01(0)	6.339	6.489	6.740	6.744	6.824	6.906	6.718	6.923	
3.81(0)	6.339	6.489	6.740	6.744	6.825	6.907	6.718	6.925	
3.24(3)	6.339	6.489	6.740	6.743	6.827	6.907	6.720	6.925	
2.59(8)	6.339	6.490	6.740	6.743	6.829	6.909	6.722	6.925	
1.94	6.339	6.489	6.740	6.743	6.830	6.909	6.725	6.922	6.993
1.33(2)	6.339	6.489	6.740	6.743	6.830	6.909	6.730	6.915	6.985
0.84				6.744	6.829	6.908	6.733	6.903	6.974
0.42				6.746	6.826	6.905	6.738	6.879	6.948
0.16	6.339	6.489	6.740	6.747	6.823	6.902	6.743	6.850	6.926
0.05				6.748	6.819	6.899	6.744	6.844	6.927
0.01				6.749	6.818	6.899	6.718	6.923	

Table 3. Binding constants and their absolute errors for experiments of **1a** with acid (2 – TfOH, 6 – HCl) measured in CD₃CN.

Experiment nr	K_d (M ⁻¹)		
	H ₃	H ₈	H ₆
1	$(3.0 \pm 0.6) \cdot 10^3$	$(1.5 \pm 1.1) \cdot 10^4$	$(4.4 \pm 1.9) \cdot 10^3$
6	168 ± 3.8	$(1.4 \pm 0.2) \cdot 10^3$	-

The Bindfit fit for experiment 2 for signal H₃ can be found here: [link](#)

The Bindfit fit for experiment 2 for signal H₈ can be found here: [link](#)

The Bindfit fit for experiment 2 for signal H₆ can be found here: [link](#)

The Bindfit fit for experiment 6 for signal H₃ can be found here: [link](#)

The Bindfit fit for experiment 2 for signal H₃ can be found here: [link](#)

* Although Bindfit fits were conducted in this thesis, their data cannot be used as an indicator of self-assembly of **1a** due to the multiple interactions of acid and solvent.

Appendix 2. Colour Changes During the Experiments 3 and 4

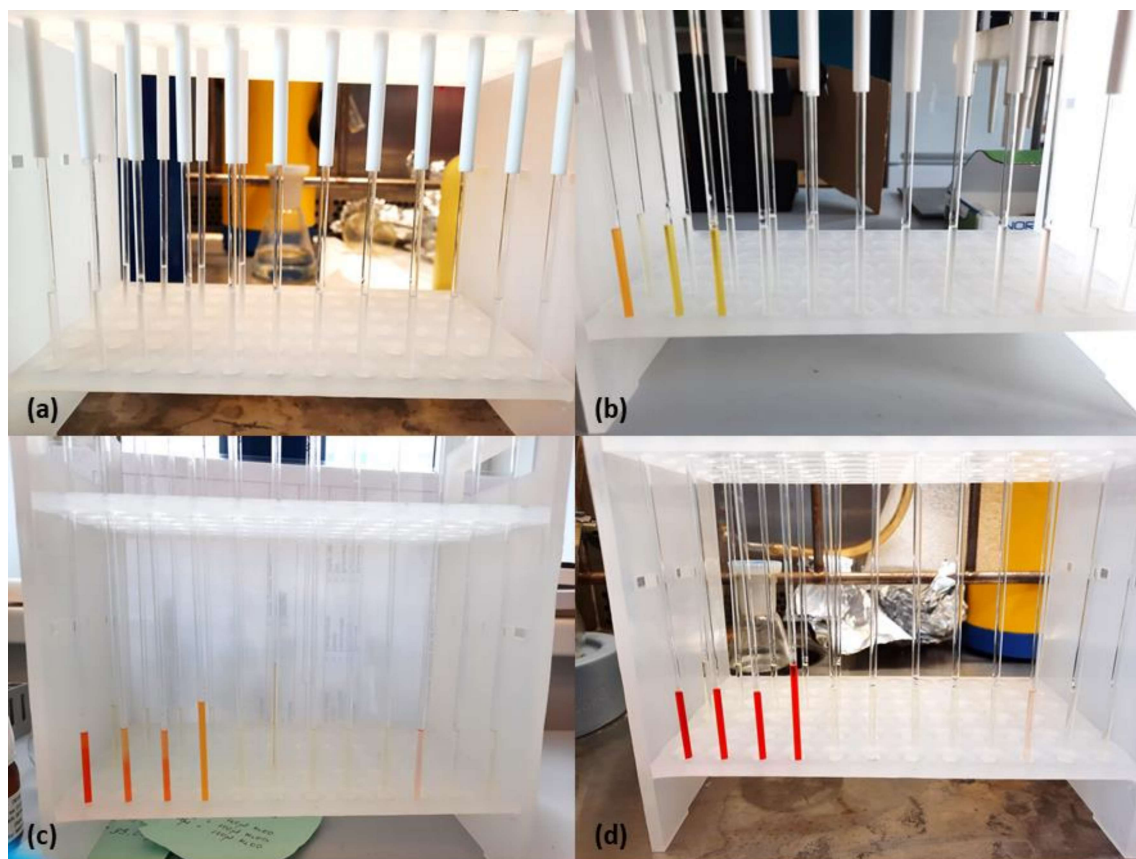


Figure 32. (a) Samples for experiment 3 where 2.5 μl of TfOH was added to the **1a** and CD_3CN stock solution. Acid made previously yellow stock solution colourless. (b) Colour changes of the samples after seven days of adding an additional 7.5 μl of TfOH to measure experiment 4 (6 days after initial acid addition). (c) Samples after 14 days from the first acid addition for experiment 3. (d) Samples after a month from initial acid addition.

Appendix 3. NMR Experiment Measuring Parameters

Table 4. Measuring parameters for the NMR experiments.

Experiment notation	Measuring parameters		
	NS	D1 (s)	T (K)
1	8-328	5,1	298
2	8-328	5,1	293
3	8-64	5	298
4	8-64	5	298
5	8	5	298
6	8-328	5,1	298
7	8	5	298
8	8	5	298
9	16	1.5	298

Table 5. Dilution plan for experiments 1, 2 and 6 ^1H experiments.

Sample nr	Concentrations of 1 solutions (mM)	Concentrations of 2 and 6 solutions (mM)	Volume of previous solution (μl)	Volume of CD_3CN (μl)
0		$m(\text{C1}) = 1.275 \text{ mg}$		650
1	4.01	4.00	600	0
2	3.81	3.80	570	30
3	3.24	3.23	510	90
4	2.59	2.58	480	120
5	1.94	1.94	450	150
6	1.33	1.32	410	190
7	0.84	0.84	380	220
8	0.42	0.42	300	300
9	0.16	0.16	235	365
10	0.05	0.05	175	425
11	0.01	0.01	126	474

Table 6. Dilution plan for experiments 3 and 4.

Sample nr	Concentration gradient (mM)	Volume of stock solution (μl)	Volume of CD_3CN (μl)
1	7.86	150	
2	7.44	142	8
3	7.02	134	16
4	6.60	126	24
5	6.18	118	32
6	5.82	111	39
7	5.40	103	47
8	4.98	95	55
9	4.56	87	63
10	4.14	79	71
11	3.72	71	79

Sample nr	Concentration gradient (mM)	Volume of stock solution (μ l)	Volume of CD ₃ CN (μ l)
12	2.88	55	95
13	2.10	40	110
14	1.26	24	126
15	0.84	16	134
16	0.42	8	142
17	0.05	1	149

Table 7. Time intervals between ¹H NMR measurements for experiment 7.

Spectrum number	Time between measurements (min)
1–52	4.5
53–64	10
65–80	15
81–92	20
93–106	30

Non-exclusive Licence for Publication and Reproduction of Graduation Thesis

I Kirsti Palmi (date of birth: 19.02.91)

1. grant Tallinn University of Technology free licence (non-exclusive licence) for my thesis An Investigation of the Self-Association Behaviour of Novel Lipophilic Fluorophores in Acidic Conditions with NMR Spectroscopy supervised by Jasper Adamson and Helena Vanessa Roitmeyer to be

1.1 reproduced for the purposes of preservation and electronic publication, incl. to be entered in the digital collection of TUT library until expiry of the term of copyright;

1.2 published via the web of Tallinn University of Technology, incl. to be entered in the digital collection of TTÜ library until expiry of the term of copyright.

2. I am aware that the author also retains the rights specified in clause 1.

3. I confirm that granting the non-exclusive licence does not infringe third persons' intellectual property rights, the rights arising from the Personal Data Protection Act or rights arising from other legislation.

(signature)

(date)